# DEVELOPMENT OF IMMUNOSENSOR BASED ON PIEZOELECTRIC QUARTZ CRYSTAL MICROBALANCE FOR *Vibrio cholerae* O1 DETECTION

**WARARAT CHONGPERMPORNWATTANA**

**A THESIS SUBMITTED IN PARTIAL FULFILLMENT**
**OF THE REQUIRMENTS FOR**
**THE DEGREE OF MASTER OF ENGINEERING**
**(BIOMEDICAL ENGINEERING)**
**FACULTY OF GRADUATE STUDIES**
**MAHIDOL UNIVERSITY**
**2006**

**ISBN 974-04-7873-5**

Thesis
Entitled

# DEVELOPMENT OF IMMUNOSENSOR BASED ON PIEZOELECTRIC QUARTZ CRYSTAL MICROBALANCE FOR *Vibrio cholerae* O1 DETECTION

Wararat Chongpermpornwattana
.....
Miss. Wararat Chongpermpornwattana
Candidate

.....
Asst. Prof. Chatchai Neatpisarnvanit,
Ph.D. (Electrical Engineering)
Major-Advisor

.....
Asst. Prof. Chamras Promptmas,
Ph.D. (Biochemistry)
Co-Advisor

.....
Prof M.R. Jisnuson Svasti, Ph.D.
Dean
Faculty of Graduate Studies

Theeraporn Rubcumintara
.....
Asst. Prof. Theeraporn Rubcumintara,
Ph.D. (Materials Engineering & Science)
Chair
Master of Engineering Programme in
Biomedical Engineering
Faculty of Engineering

Thesis
Entitled

# DEVELOPMENT OF IMMUNOSENSOR BASED ON PIEZOELECTRIC QUARTZ CRYSTAL MICROBALANCE FOR *Vibrio cholerae* O1 DETECTION

was submitted to the Faculty of Graduate Studies, Mahidol University
for the degree of Master of Engineering (Biomedical Engineering)
on
November 1, 2006

Wararat Chongpermpornwattana
Miss Wararat Chongpermpornwattana
Candidate

Asst. Prof. Bovornlak Oonkhanond,
Ph.D. (Chemical Engineering)
Chair

Asst. Prof. Chatchai Neatpisarnvanit,
Ph.D. (Electrical Engineering)
Member

Asst. Prof. Udom Tipayamontri,
Ph.D. (Physiology)
Member

Asst. Prof. Chamras Promptmas,
Ph.D. (Biochemistry)
Member

Prof. M.R. Jisnuson Svasti, Ph.D.
Dean
Faculty of Graduate Studies
Mahidol University

Asst. Prof. Piya Rattanasuwan,
M.Eng.
Dean
Faculty of Engineering
Mahidol University

# ACKNOWLEDGEMENTS

I am wholeheartedly grateful for the help, encouragement and advice from my advisor, Asst. Prof. Chatchai Neatpisarvanit throughout my thesis work.

I would like to express my sincere gratitude and deepest appreciation to my co-advisor, Asst. Prof. Chamras Promptmas for his help and kindness in giving comments and advice on the thesis work.

I also appreciate the help from Dr. Sureerat Porntadavity in the Department of Clinical Chemistry, Faculty of Medical Technology, Mahidol University, Thailand.

Sincere appreciation is expressed to my teacher, Asst. Prof. Ittichote Chuckpaiwang in the Department of Mechanical Engineering, Faculty of Engineering, Mahidol University, Thailand.

I would like to thank all friends and staff in Department of Biomedical Engineering, Faculty of Engineering, Mahidol University, Thailand.

I wish to thank the staff in Department of Clinical Chemistry and Department of Clinical Microbiology, Faculty of Medical Technology, Mahidol University, Thailand for their friendly assistance.

Finally, I would like to express my gratitude to my parents, my family, and my friends for their infinite love, attention, understanding and encouragement which will never be forgotten.

Wararat Chongpermpornwattana

DEVELOPMENT OF IMMUNOSENSOR BASED ON PIEZOELECTRIC QUARTZ CRYSTAL MICROBALANCE FOR *VIBRIO CHOLERAE* O1 DETECTION

WARARAT CHONGPERMPORNWATTANA 4636077 EGBE/M

M.Eng.(BIOMEDICAL ENGINEERING)

THESIS ADVISORS: CHATCHAI NEATPISARNVANIT, Ph.D. (Electrical Engineering), CHAMRAS PROMPTMAS, Ph.D. (Biochemistry)

## ABSTRACT

Cholera is an major acute diarrheal disease presenting with severe watery diarrhea. The cholera bacteria usually contaminate by food and water. Rapid detection is necessary for effective control of this disease.

The piezoelectric immunosensor (PZ) based on specific antigen-antibody binding has rapidly been developed due to its increasing importance in the diagnosis of disease. PZ immunosensor has been used for *V. cholerae* O1 detection, due to its sensitivity, specificity, low cost, portability and suitability for direct and label-free monitoring. The aim of this study is to develop a QCM system for *V. cholerae O1* detection.

A gold electrode of 12 MHz AT-cut quartz crystal was coated with protein A. Then, anti-*V. cholerae* O1 was immobilized on the crystal surface. Subsequently, prepared QCM was dipped into *v. cholerae* O1 suspension. The binding between anti-*V. cholerae* O1 and *V. cholerae* O1 decreased the frequency generated from the quartz crystal. The decreasing oscillation frequency was monitored as an indicator of *V. cholerae* O1.

The optimal concentration of coated protein A on the crystal surface was 1 mg/ml, incubated overnight at $4\,^{o}C$ in a moist chamber. The optimal incubation time and concentration of anti-*V. cholerae* O1 were 2 hours on the crystal surface at room temperature and 0.05 mg/ml for immobilization, respectively. The rotation technique made the anti-*V. cholerae* O1 –*V. cholerae* O1 binding to better. The estimated lower detection limit for *V. cholerae* O1 was approximately $10^4$ CFU/ml. In contrast to the conventional microbiological culture, the proposed technique based on piezoelectric quartz crystal microbalance is faster. This PZ immunosensor system offered higher sensitivity and specificity and is therefore suitable for *V. cholerae* O1 detection.

KEY WORDS : PIEZOELECTRIC / IMMUNOSENSOR / *VIBRIO CHOLERAE* O1 / SAUERBREY EQUATION / ACOUSTIC WAVE / QUARTZ CRYSTAL MICROBALANCE

95 P. ISBN 974-04-7873-5

การพัฒนาอิมมูโนเซ็นเซอร์โดยอาศัยหลักการเพียโซอิเลคทริคในการตรวจหาเชื้อ *Vibrio cholerae* O1
(DEVELOPMENT OF IMMUNOSENSOR BASED ON PIEZOELECTRIC QUARTZ CRYSTAL MICROBALANCE FOR *VIBRIO CHOLERAE* O1 DETECTION)

วรารัตน์ จงเพิ่มพรวัฒนา 4636077 EGBE / M

วศ.ม.(วิศวกรรมชีวการแพทย์)

คณะกรรมการควบคุมวิทยานิพนธ์: ฉัตรชัย เนตรพิศาลวนิช, Ph.D. (Electrical Engineering), จำรัส พร้อมมาศ, Ph.D. (Biochemistry)

บทคัดย่อ

อหิวาตกโรคเป็นโรคที่ก่อให้เกิดอาการอุจจาระร่วงอย่างเฉียบพลัน สาเหตุมาจากเชื้อของ *Vibrio cholerae* ซึ่งปนเปื้อนทางอาหารและน้ำดื่ม การตรวจหาเชื้อดังกล่าวได้อย่างรวดเร็วมีความสำคัญยิ่งในการควบคุมการแพร่ระบาด

เพียโซอิมมูโนเซ็นเซอร์อาศัยหลักการจับกันระหว่างแอนติเจนกับแอนติบอดีอย่างจำเพาะเจาะจง มีการพัฒนาอย่างรวดเร็วในการช่วยวินิจฉัยโรค เพียโซอิมมูโนเซ็นเซอร์เป็นไบโอเซ็นเซอร์ชนิดหนึ่ง ที่นำมาใช้ในการตรวจหาเชื้อแบคทีเรียชนิดนี้ มีความไวและความจำเพาะเจาะจงสูง ราคาถูก พกพาได้ และสามารถใช้ตรวจหาเชื้อได้โดยตรง โดยไม่ต้องติดฉลากเพื่อทำการวัด จุดมุ่งหมายในการศึกษานี้คือการพัฒนาเครื่องอิมมูโนเซ็นเซอร์โดยอาศัยหลักการเพียโซอิเลคทริคในการตรวจหาเชื้อ *Vibrio cholerae* O1

ในการศึกษาครั้งนี้ทำการเตรียมควอทซ์อิเลคโทรดโดยฉาบด้วยโปรตีนเอแล้วตรึงด้วย anti-*V. cholerae* O1 บนผิวของควอทซ์ หลังจากเตรียมควอทซ์แล้ว จึงจุ่มลงในสารละลายที่มีเชื้อนี้อยู่ การจับกันระหว่าง anti-*V. cholerae* O1—*V. cholerae* O1 มีผลให้ความถี่ของควอทซ์ที่ลดลง ความถี่ที่ลดลงสามารถบ่งชี้ถึงปริมาณแบคทีเรียได้

จากการศึกษาความเข้มข้นของโปรตีนเอ และแอนติบอดี ที่เหมาะสมในการทดลองนี้พบว่าโปรตีนเอความเข้มข้น 1 มิลลิกรัมต่อมิลลิลิตร หยดบนควอทซ์ตลอดคืนที่อุณหภูมิ 4 องศาเซลเซียส ในกล่องเก็บความชื้น แอนติบอดีที่ความเข้มข้น 0.05 มิลลิกรัม ต่อ มิลลิลิตร และตรึงบนผิวควอทซ์ นาน 2 ชั่วโมงจะให้ค่าความถี่ที่เปลี่ยนแปลงสูงที่สุด นอกจากนั้นการเคลื่อนที่แบบหมุนช่วยเพิ่มการจับกันของ anti-*V. cholerae* O1—*V. cholerae* O1 ได้ดียิ่งขึ้น จากผลการทดลองพบว่าเซ็นเซอร์นี้สามารถตรวจวัดเชื้อ *V. cholerae* O1 ได้ถึงสูงถึง $10^4$ CFU (colony forming unit) ต่อมิลลิลิตร เมื่อทำการเปรียบเทียบกับวิธีการเลี้ยงเชื้อในห้องทดลอง พบว่าเพียโซอิเลคทริคอิมมูโนเซ็นเซอร์สามารถตรวจวัดได้รวดเร็วกว่า พร้อมทั้งมีความไวและความจำเพาะเจาะจงในการตรวจวัดที่สูงกว่า ดังนั้นจึงเหมาะสมในการตรวจวัด *V. cholerae* O1

95 หน้า ISBN 974-04-7873-5

# CONTENTS


| | | Page |
|---|---|---|
| **ACKNOWLEDGEMENT** | | iii |
| **ABSTRACT** | | iv |
| **LIST OF FIGURES** | | ix |
| **LIST OF ABBREVIATIONS** | | xi |
| **CHAPTER** | | |
| **I** | **INTRODUCTION** | |
| | 1.1 Motivation | 8 |
| | 1.2 Objectives | 8 |
| | 1.3 Scope of Work | 8 |
| | 1.4 Expected Results | 9 |
| | 1.5 Thesis Organization | 9 |
| **II** | **LITERATURE REVIEW** | 11 |
| | 2.1 Electronic Development Phase | 11 |
| | 2.1.1 Basic Piezoelectric Resonators | 11 |
| | 2.1.2 Piezoelectric Quartz Crystal Microbalance (QCM) | 12 |
| | 2.1.3 Measuring System | 19 |
| | 2.2 Biological Development Phase | 23 |
| | 2.2.1 Immobilization of Antibodies | 23 |
| | 2.2.2 Evaluation of Affinity Interaction | 28 |
| **III** | **METHODOLOGY** | 33 |
| | 3.1 Materials | 33 |
| | 3.1.1 Reagents and Microorganism | 33 |
| | 3.1.2 Instruments | 34 |

# CONTENTS

**(continued)**


| | | Page |
|---|---|---|
| | 3.1.3 Laboratory Equipment | 34 |
| | 3.1.4 Sample for Bacterial Extraction | 35 |
| | 3.1.5 Preparation of Reagents | 35 |
| | 3.2 Methods | 36 |
| | 3.2.1 Electronic Development Phase | 36 |
| | 3.2.2 Biological Development Phase | 40 |
| | 3.2.2.1 Preparation of Quartz Crystal Microbalance | 40 |
| | 3.2.2.2 Study the Optimal Detection Condition | 41 |
| | 3.2.2.2.1 Optimization of Protein A Concentration | 41 |
| | 3.2.2.2.2 Determination of Response *V. cholerae* O1 to Anti-*V. cholerae* O1 | 42 |
| | 3.2.2.2.3 Determination of Optimal Incubation Time of Anti-*V. cholerae* O1 | 46 |
| | 3.2.2.2.4 Study of binding between Anti-*V. cholerae* O1 and *V. cholerae* O1 by Rotating Method | 46 |
| | 3.2.2.2.5 Optimization of Anti-*V. cholerae* O1 Concentration | 46 |
| | 3.2.2.3 Detection of *V. cholerae* O1 by Piezoelectric Immunosensor | 50 |
| **IV** | **RESULTS** | 54 |
| | 4.1 Determination of Optimal Condition for Protein A Coating | 54 |
| | 4.2 Determination of Optimal Conditions for Immobilizing Antibodies of *V. cholerae* O1 | 56 |
| | 4.2.1 Optimal Incubation Time of Anti-*V. cholerae* O1 | 56 |
| | 4.2.2 Anti-*V. cholerae* O1 and *V. cholerae* O1 Interaction by Rotating Method | 58 |
| | 4.2.3 Optimization of Anti-*V. cholerae* O1 | 61 |

# CONTENTS

**(continued)**


| | | Page |
|---|---|---|
| | 4.2.4 Optimization of Anti-*V. cholerae* O1 (continue) | 61 |
| | 4.3 Detection of *V. cholerae* O1 by Piezoelectric Immunosensor | 64 |
| **V** | **DISCUSSION** | 66 |
| | 5.1 Electronic Development Phase | 66 |
| | 5.2 Biological Development Phase | 68 |
| | 5.2.1 The Optimal Conditions for Protein A Coating | 68 |
| | 5.2.2 The Optimal Conditions for Immobilization Anti-*V. cholerae* O1 | 69 |
| | 5.2.2.1 Anti-*V. cholerae* O1 and *V. cholerae* O1 reaction | 69 |
| | 5.2.2.2 The Optimal Incubation Time of Anti-*V. cholerae* O1 | 70 |
| | 5.2.2.3 Anti-*V. cholerae* O1 and *V. cholerae* O1 Interaction by Rotating Method | 72 |
| | 5.2.2.4 The optimization of Anti-*V. cholerae* O1 | 72 |
| | 5.2.3 Detection of *V. cholerae* O1 by Piezoelectric Immunosensor | 73 |
| | 5.2.4 Comparing between Piezoelectric Immunosensor and Other Methods for *V. cholerae* O1 Detection | 74 |
| **VI** | **CONCLUSION** | 75 |
| **REFERENCES** | | 76 |
| **APPENDIX** | | 85 |
| **BIOGRAPHY** | | 95 |

# LIST OF FIGURES


| Figure | Page |
|---|---|
| 1.1 Higher power scanning electron micrograph of vibrios | 2 |
| 1.2 Structure of an antibody molecule | 4 |
| 1.3 The *Y* -shaped immunoglobulin molecule | 5 |
| 1.4 Principle of operation of a typical biosensor | 6 |
| 1.5 Concentration ranges measured by various types of biosensors and immunoassays | 6 |
| 2.1 A typical acoustic/piezoelectric sensing process | 13 |
| 2.2 Schematic sketches of the four common types of acoustic resonators and their wave propagation modes | 14 |
| 2.3 Piezoelectric quartz crystal microbalance | 16 |
| 2.4 Side cross-sectional diagram of a QCM with biofilm coated | 18 |
| 2.5 Cross sectional view of quartz crystal microbalance | 19 |
| 2.6 Measuring system of piezoelectric biosensor | 20 |
| 2.7 Oscillating circuit of Skaldal (74LS320) | 21 |
| 2.8 Oscillating circuit by CMOS inverter (MC14049) | 21 |
| 2.9 Photograph of the experimental setup of CRP sensor II | 22 |
| 2.10 Chemical compound coated on crystal surface | 26 |
| 2.11 Formation of the antigen-antibody complex | 29 |
| 2.12 Characterization of kinetic properties of antibodies | 31 |
| 3.1 Pierce crystal oscillator | 38 |
| 3.2 Piezoelectric dry analysis system | 39 |
| 3.3 Dessicator | 41 |
| 3.4 The method of coating protein A | 43 |
| 3.5 Effecting of protein A to anti- *V. cholerae* O1 immobilization on the quartz surface | 44 |

# LIST OF FIGURES

**(continued)**


| **Figure** | **Page** |
|---|---|
| 3.6 Agglutination of antigen-antibody | 45 |
| 3.7 Schematic diagram of anti- *V. cholerae* O1 on the quartz surface | 48 |
| 3.8 Systematic processes of coating method for anti- *V. cholerea* O1 on the quartz surface | 49 |
| 3.9 Schematic diagram of an immunosensor device | 51 |
| 3.10 Schematic diagram of experiment | 52 |
| 4.1 Protein A immobilization at different concentrations of protein A | 55 |
| 4.2 Optical microscopic observation (x100) of agglutination reaction | 57 |
| 4.3 Frequency shift as a function of time during immobilization of anti-*V. cholerea* O1 onto gold electrode surface of QCM | 59 |
| 4.4 Comparison of *v. cholerae* O1 binding to immobilized with and without rotation | 60 |
| 4.5 Frequency shift as a function of time during immobilization of anti-*V. cholerea* O1 ranging from 0.05 to 0.200 mg/ml | 62 |
| 4.6 Frequency shift as a function of time during immobilization of anti-*V. cholerea* O1 ranging from 0.0125 to 0.0500 mg/ml | 63 |
| 4.7 QCM sensor | 65 |
| 5.1 Protein A coating | 71 |
| 5.2 Antigen-antibody binding | 71 |

# LIST OF ABBREVIATIONS

| | | |
|---|---|---|
| $^{o}A$ | = | amstrong |
| ATP | = | adenosine triphosphate |
| cAMP | = | 3’5’-cyclic adenosine monophosphate |
| CFU | = | colony forming unit |
| CT | = | clolera toxin |
| $^{o}C$ | = | degree celcius |
| g | = | gram |
| h | = | hour |
| Da | = | dalton |
| L | = | liter |
| M | = | molar |
| $\mu l$ | = | microliter |
| mg | = | milligram |
| min | = | minute |
| ml | = | milliliter |
| ng | = | nanogram |
| PCR | = | polymerase chain reaction |
| ELISA | = | enzyme linked immunosorbent assay |
| psi | = | pound per square inch |
| sec | = | second |
| PZ | = | piezoelectric |
| QCM | = | quartz crystal microbalance |
| Ab | = | antibody |
| Ag | = | antigen |
| Hz | = | Hertz |
| BAW | = | bulk-acoustic wave |

# LIST OF ABBREVIATIONS

**(continued)**

| | | |
|---|---|---|
| TSM | = | thickness-shear-mode |
| FPW | = | flexural-plate-wave |
| SAW | = | surface-acoustic-wave |
| N | = | newton |
| AFP | = | alpha-fetoprotein |
| CRP | = | C-reactive protein |
| HSA | = | human serum albumin |
| PTFE | = | polytetrafluoroethylene or Teflon |
| IgG | = | immunoglobulin G |
| TB | = | Tuberculosis |
| BSA | = | bovine serum albumin |
| SAM | = | self-assembled monolayer |
| GND | = | ground |
| DW | = | distilled water |
| PBS | = | phosphate buffer saline |
| RT | = | room temperature |
| V | = | volt |

# CHAPTER I
# INTRODUCTION

The genus Vibrio includes at least 20 species. *Vibrio cholerae* O1 is one kind of bacteria species causing an epidemic and life-threatening secretory diarrhea by food and water contamination. The patient's symptom is voluminous watery stools and numerous vomiting resulting in hypovolumic shock and acidosis. Vibrios are Gram-negative bacteria, highly motile curved rods with a single polar flagellum as shown in Fig. 1.1 [1]. Isolation of vibrio can grow readily on most ordinary media but enrichment and selective media are necessary for faeces and other material containing mixed flora. The colonies may be opaque or translucent, flat or domed, hemolytic or non-hemolytic, smooth or rough. [2].

Pathogenesis of cholera is transmitted by the fecal-oral route. Vibrios are sensitive to acid, so most of them die in the stomach. *Vibrio cholerae* adheres to and multiplies on the epithelial cell that lines the small intestine but it does no visible damage to them. However, this vibios produces a potent enterotoxin (an exotoxin that acts on the intestine) choleragen, which is responsible for the symptoms of cholera. As with a number of other bacterial exotoxins, choleragen is heat labile (inactivated by heat) and its protein molecule is composed of two parts; $A$ and $B$. The $B$ fragment has no toxic activity but binds irreversibly to specific receptors on the microvilli of the intestinal cell. The $A$ fragment, responsible for toxicity, causes the activation of the enzyme adenylate cyclase, which converts adenosine triphosphate (ATP) to cyclic adenosine monophosphate (cAMP). Accumulation of cAMP in the cell causes a markedly increased secretion of water and electrolytes. Although the colon is not toxin, it cannot absorb the huge volume of fluid that rushes through it so diarrhea results will be presented. The normal shedding of intestinal cells eventually gets rid of the toxin. Therefore, the patients have diarrhea and vomit, the major symptom of

cholera toxin (CT). Cholera is epidemic disease in undeveloped countries because of raw cooking and non -sterile food. There have been seven cholera pandemics since the early 1800s.

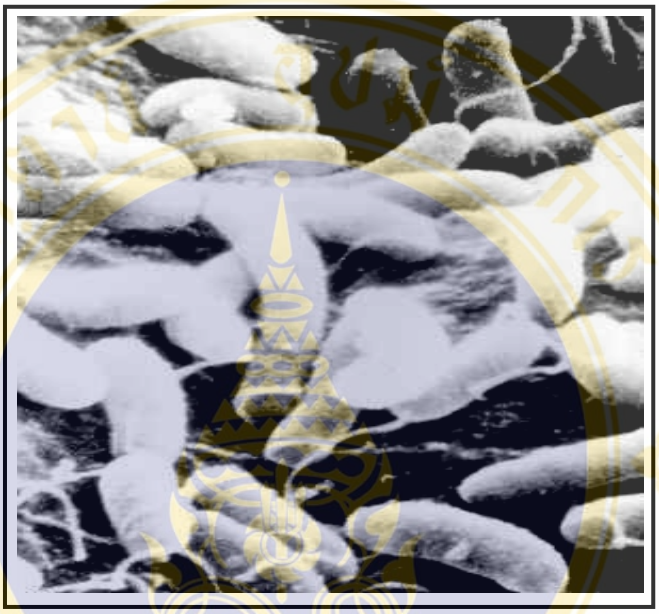

**Figure 1.1** Higher power scanning electron micrograph showing single polar flagellum of the vibrios [1].

Treatment of cholera depends on the rapid replacement of salts and water before irreversible damage to vital organs will occur. The prompt administrations of intravenous or oral dehydration fluid decreases the mortality of cholera to less than 1%. Antibiotic therapy limits the duration of the illness somewhat, but the primary concern is replacement of lost fluids. Therefore, the doctors can diagnosis vibrios rapidly helping the patients' life [4].

Diagnosis of *v. cholerae* O1 is wet mount of liquid stool by microscopy. Other methods are culture of stool and rectal swab sample on cultured media for 2-7 days. Recently the polymerase chain reaction (PCR) and genetically-based rapid techniques have been recommended for use in specialized laboratories [1]. Most methods are

slow in diagnosis. Furthermore, these methods must be analyzed by highly skilled technician. At the present, scientists try to develop modern techniques for using *v. cholerae* O1 detection.

Basically, immunoassays are analytical tests that utilize antibodies (Ab). Antibodies are the molecules of the specific immune system, and its molecule has two separate functions: one is to bind specifically to molecules from the pathogen that elicited the immune response; another is to recruit other cells and molecules to destroy the pathogen once the antibody is bound to it. These functions are structurally separated in the antibody molecule, one part of which recognizes and binds to the pathogen or antigen whereas another part engages different effecter mechanisms. The antigen-binding site varies extensively between antibody molecules. Thus, this site is known as the variable region or $V$ region. The variable region consists of the $NH_3$ or ammonia group at the end of a peptine chain, so this region is usually called $N$ terminus. The region of the antibody molecule does not vary in the same way. This region is known as the constant region or $C$ region. The $C$ region composes of the $COOH$ or carboxyl group at the last part of peptine chain, so other name is called $C$ terminus as shown in Fig. 1.2 [5]. Antibody molecules are roughly $Y$-shaped molecules consisting of three equal-sized portions, connected by a flexible tether. Three schematic representation of antibody structure has been determined by $X$-ray crystallography. The antibody can be digested with photolytic enzymes (proteases) that cleave polypeptide sequences so the digestion technique could be used to dissect the structure of antibody molecules and to determine which parts of the molecule are responsible for its various functions as shown in Fig. 1.3. Two fragments are identical and contain the antigen-binding activity, $F_{ab}$. These are termed the $F_{ab}$ fragments or antigen binding fragment. The other fragment contains no antigen-binding activity but was crystallized, $F_c$. When pathogens (antigen) contaminate to human body, the immune system will produce antibodies to attach pathogens and to remove them from the body. An antibody generally recognizes only a small region on the surface of a large molecule such as a polysaccharide or protein. The structure recognized by an antibody is called an antigenic determinant or epitope. $F_{ab}$ of antibody binds to some

sequences of antigen specifically, thus the formation of antigen-antibody complex occurs.

From knowledge of immunoassay, the scientists apply the medical instrument called "*biosensor*". It is composed of two important parts; a recognition and transducer parts. The recognition part is a biological sensing element (receptor) on the surface of biosensor, for example, an antibody, enzyme, or DNA. Another, transducer, converts the analyte-receptor reaction into a quantitative electrical signal as shown in Fig. 1.4 [7]. Transducers could detect signal based on optical, thermal, electrical, or electronic elements. The detected signal is highly specific for the analyte of interest and able to respond to the appropriate concentration range [8]. Moreover, transducer should have moderately fast response time (1-60 sec) and suitable device [7-15].

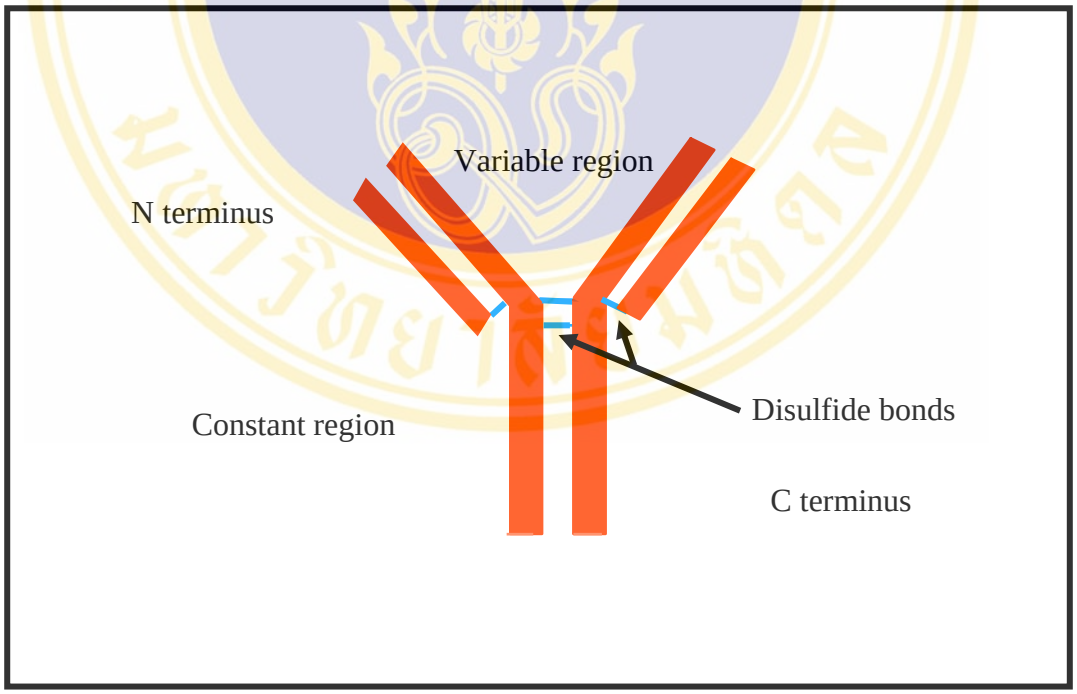


**Figure 1.2** Structure of an antibody molecule consists of the variable region the constant region, and the disulfide bond [5].

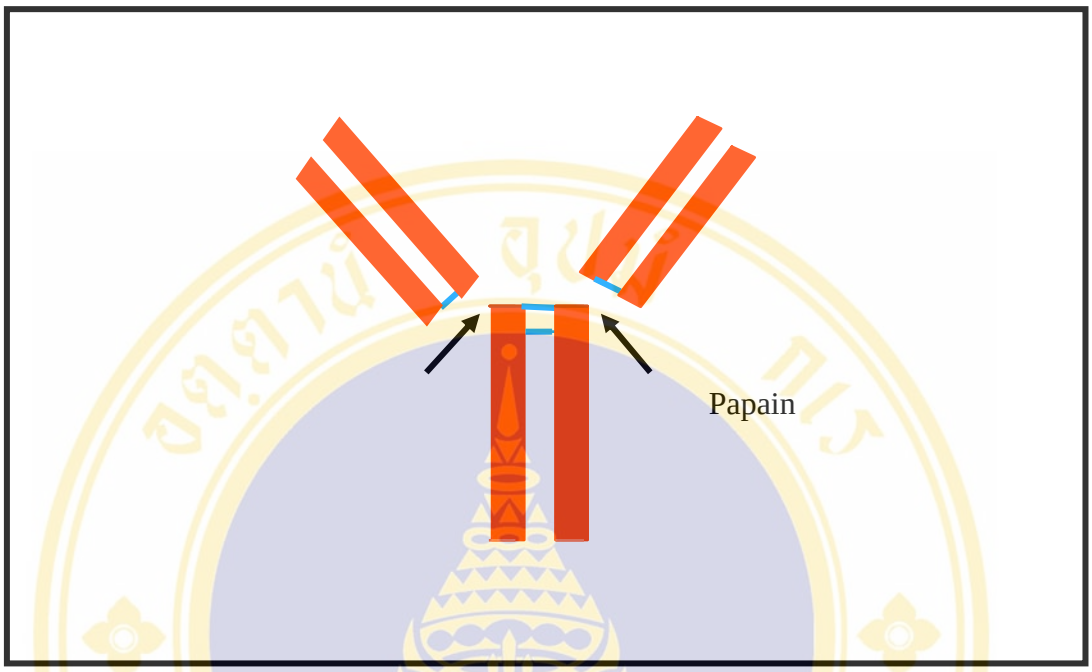


**Figure 1.3** The $Y$-shaped immunoglobulin molecule can be dissected by partial digestion with proteases: papain cleaves the immunoglobulin molecule into three pieces, two $F_{ab}$ fragments and one $F_c$ fragment. $F_{ab}$ contains the $V$ regions and binds antigen. The $F_c$ fragment is cystallizable and contains $C$ regions [6].

Properties of a biosensor in the design consist of specificity, sensitivity, reproducibility, stability, regenerability, and response time. The specificity and sensitivity is the most important of prior biosensor development [17-19]. The antigen-antibody biosensor or immunosensor has a much higher specificity than the average chemical sensor, and this advantage needs to be exploited. Figure 5 shows the relative concentration ranges that measure using enzyme electrode and immunoassay sensors. The antigen-antibody-based biosensors can detect analytes at lower concentration ranges [20-23].

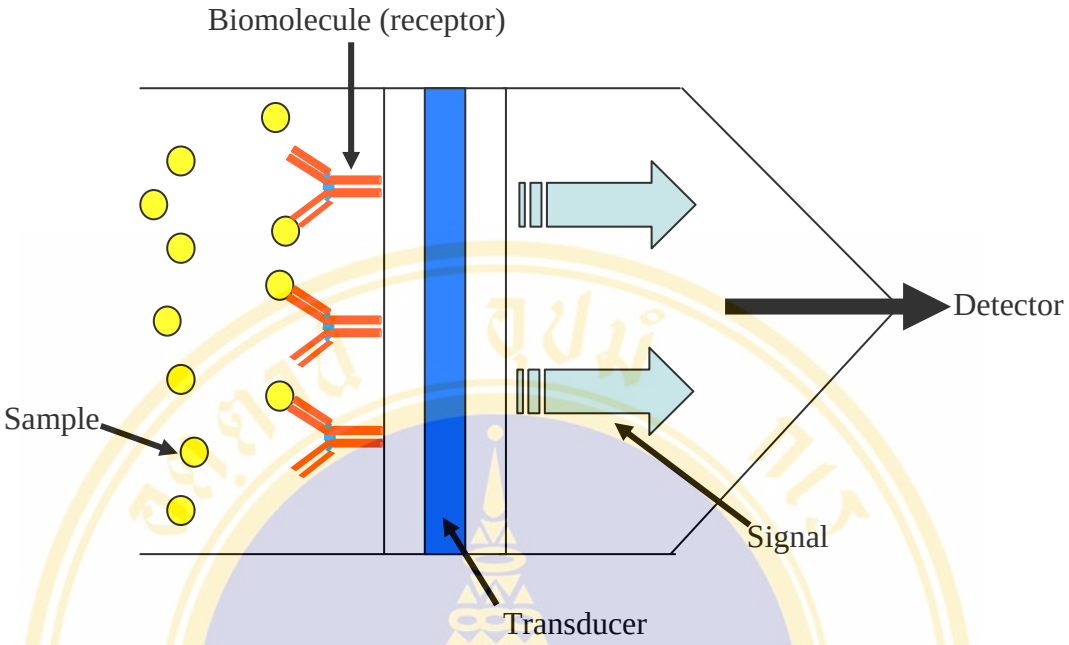


**Figure 1.4** Principle of operation of a typical biosensor. When samples bind to the biomolecule (receptor) sensing part on the surface of biosensor, transducers will converts the analyte-recepter reaction in to a quantitative electrical signal through detector [7].

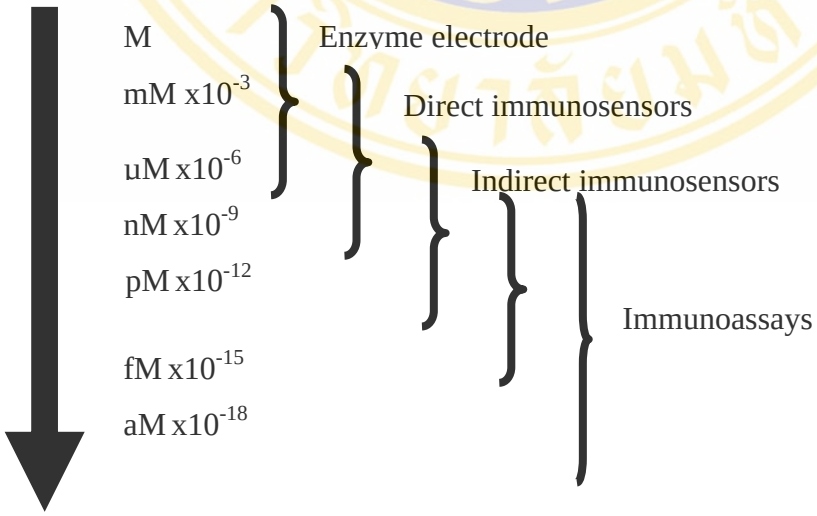


**Figure 1.5** Concentration ranges measured by various types of biosensors and immunoassays [20].

Use of both qualitative and quantitative analysis has proved to be one of the most productive technologies in medicine and immunological researches. Traditional immunoassays are based on the enzyme, fluorescent, or radioactive element-labeled second antibodies and associated substrates to generate the final signal. Immunosensor system combines with a transducer to detect chemicals *in vivo* or *in vitro* or producing a response after a specific interaction with the chemicals. The combination of the physical transducer with the immunoreactions bring about a new generation of immunoassay devices, which are small, self-contained, specific, cheap, and robust. Types of immunosensors include potentiometric, optical, amperometric, and piezoelectric (PZ) crystal devices. These transducers convert immunoreaction events into different physical signals and can be sensitive to antigen (Ag)/ antibody (Ab) concentrations. Although mostly advanced optical systems are utilized, the piezoelectric and acoustic devices represent similar but significantly less expensive alternative. This thesis should provide a better insight into piezoelectric sensors with respect to bioanalytical applications.

Piezoelectric (PZ) biosensor is very attractive because it has many advantages. Piezoelectric biosensor offers a real-time output, simplicity of use and reasonable cost. Many reports have been published using PZ for a wide range of applications in the food industry, environmental monitoring, clinical diagnostics and biotechnology. The general PZ-idea is based on coating the crystal surface with a selectively binding substance such as antibodies to bacteria. Bacteria will bind to the antibodies specifically. Mass on crystal will increase while the resonance frequency of oscillation will decrease proportionally [24-27]. Some recent example of PZ biosensors are presented below.

In 1992, Plomer *et al* [28] reported that piezoelectric immunosensor could detect *Escherichia coli* O157:H7. This bacteria causes virulent diarrhea. The proposed sensor could discover *E. coli* within 30-50 min. In-Seon Park *et al* [29] improved antibody-coated sensor system on quartz crystal for detection of *Salmonella* spp. causing diarrhea. They used thiolate group to immobilize antibodies on the crystal surface. Thiolate group resulted in sensitivity and stability of antibodies. In 2002, a report by Shu-Fen Chou *et al* [30] was published about measuring $\alpha$-fetoprotein (AFP) with

piezoelectric biosensor. Increased AFP in adult plasma was considered an early indication of hepatocellular carcinoma and teratoblastoma.

## 1.1 Motivation

Piezoelectric immunosensors are appropriate instruments for detecting microorganisms especially bacteria. This thesis develops immunosensor based on piezoelectric for *v. cholerae* O1 detection because conventional vibrios method has many problems. There are two conventional methods. The first method called culture method is time-comsuming (2-7 days), low accuracy and precision process. The second method is the Polymerase Chain Reaction (PCR) method which also requires highly skilled microbiological laboratory technicians. PCR method requires expensive chemical reagent and equipment. This thesis considers many advantages of piezoelectric immunosensor for *v. cholerae* O1 detection. Piezoelectric immunosensors can offer rapid detection, high specificity and low cost.

## 1.2. Objectives

The main objective of this research is to study and verify appropriate procedure implementing piezoelectric immunosensor in *vibrio cholerae* O1 detection. To be specific, the mission is to develop coating process of polyclonal antibody on the QCM. Furthermore, this research aims to develop high sensitivity, high specificity and low cost measuring equipment. An extensive error study and statistical analysis will be used as a foundation for further development of other immunosensors based on piezoelectric for pathogen analysis.

## 1.3 Scope of work

This thesis will focus on three parts. The first part is the measuring unit of system setup. The suitable oscillator circuit and frequency counter are developed for *v. cholerae* O1 detection. The PIC microcontroller (Microchip Inc.) functions as frequency counter and oscillator circuit generating resonant frequency using the QCM device. The second part is the immobilization of anti-*V. cholerae* O1 antibodies on the QCM device. Protein A is the solid support membrane of antibody on gold crystal surface. The last part, frequency shift is calculated for *v. cholerae* O1 mass and concentration while *v. cholerae* O1 is cultured for measuring concentration. Correlation factor ( $R$ factor) of measured concentration from both methods, $R$ factor predicts sensitivity and specificity of the proposed.

## 1.4 Expected results

The proposed QCM biosensor could detect the *v. cholerae* O1 in rapid time with high sensitivity and specificity when compared with conventional methods such as bacteria culture method.

## 1.5 Thesis organization

Introduction chapter explains general *v. cholerae* O1 in feature and function of this bacterium. Moreover, the first chapter still presents about fundamental immunoassay, biosensor and piezoelectric immunosensor. Objectives, scope of work and expected results from experiment are described in this chapter. The second chapter, literature review is separated into two phases. The primary phase shows the development of construction of piezoimmunosensor and measuring system. Another phase displays biological improvement phase for immobilization process and affinity interaction of antibodies. Consequently, methodology in the third chapter consists of used materials in thesis experiment and many methods for study optimal conditions of piezoimmunosensor. Then, chapter IV is the results of optimal conditions for *v.*

*cholerae* O1 detection from all experiment. Subsequently, chapter V is discussion of choosing oscillator suitably, creating portable device, finding out the optimal conditions from scientific reasons, and developing from gas phase to liquid phase in the future. The last chapter concludes interpretation of this work and future work in the next time.

# CHAPTER II
# LITERATURE REVIEW

Review of piezoelectric immosensor is divided into two phases. The first phase was explained development construction of piezoelectric resonators and measuring system for piezosensors. Biological development phase in secondary phase, presented to immobilize antibodies on the quartz surface and to evaluate the affinity interaction.

## 2.1 Electronic Development Phase

This phase consists of the essential three parts; Basic piezoelectric resonators given details in 2.1.1, piezoelectric quartz crystal microbalance (QCM) given explanation in 2.1.2, and the measuring system given explanation in 2.1.3.

### 2.1.1 Basic Piezoelectric Resonators

From knowledge of wave theory, the scientists explained the relationship between acoustic wave sensing mechanisms and piezoelectric effect of quartz crystal microbalance in physics of wave and application of crystals. The main emphasis of this article is placed on piezoelectric resonators.

**Acoustic Wave Sensing Mechanisms**

The spectrum of acoustic waves covers 14 frequencies range from $10^{-2}$ Hz to $10^{12}$ Hz as shown in Fig.6 [31]. The acoustic resonator is a narrow frequency range of $10^{6}$ to $10^{9}$ Hz in oscillating sensors. The stress to solid results in strain (elastic deformation) to travel of waves through the solid (crystal). The type of wave depend on the crystal structure such as transversal or longitudinal and the phase velocity. In 1880, the Curie brothers previously reported piezoelectricity effect. They presented the

generation of electrical changes on the surface of a solid caused by pulling, pressure, or torsion. In contrast, the occurrence of a mechanical deformation arising from an external electric field is called the converse piezoelectric effect. The general relationships between mechanical and electrical variables are showed in Fig. 2.1 [32]. Increasing expression responses to the electrical excitation of elastic waves in a piezoelectric solid. The motion on the quartz surface causes a change in phase, which can detect electricity [33-40].

Bulk-acoustic wave (BAW) or thickness-shear-mode (TSM) resonator is also known as quartz-crystal microbalance (QCM). Although TSM resonators are less sensitive than flexural-plate-wave (FPW) or surface-acoustic-wave (SAW) sensors, they are widely used because of their robust nature, availability, and affordable electronics. Figure 8 displays the four common types of acoustic resonator and their wave propagation modes [41-47].

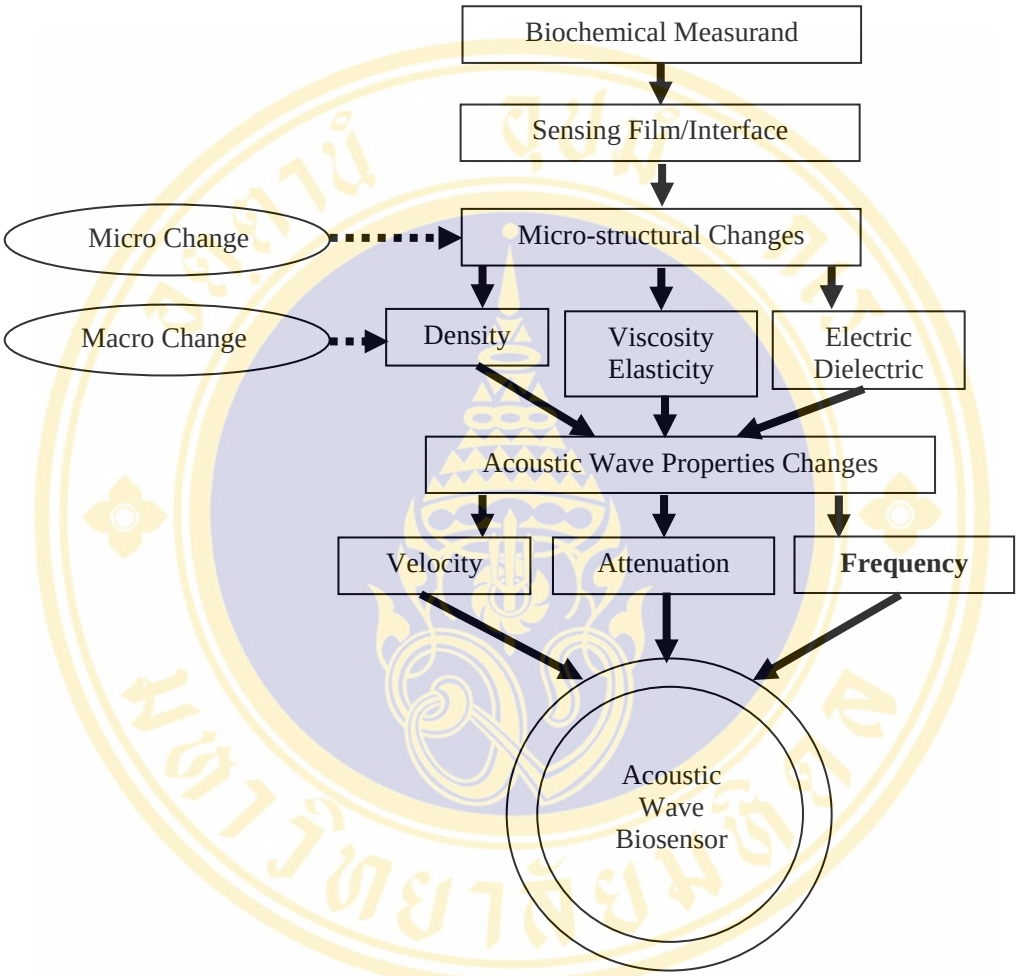


**Figure 2.1** A typical acoustic/piezoelectric sensing process [32].

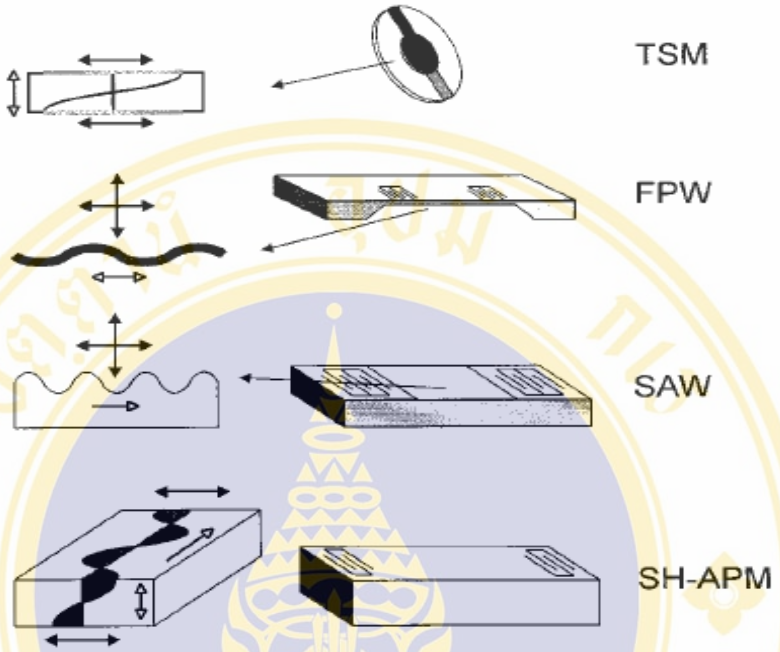


**Figure 2.2** Schematic sketches of the four common types of acoustic resonators and their wave propagation modes. The particle displacement is indicated by black arrow and the direction of the wave propagation by an open arrow. TSM: thickness-shear-mode resonator, also known as the quartz –crystal microbalance technique; FPW: flexural-plate-wave resonator; SAW: surface –acoustic-wave resonators (two port delay line) and SH-APM: shear-horizontal-acoustic-plate-mode resonator [48].

### 2.1.2 Piezoelectric Quartz Crystal Microbalance (QCM)

In 1885, Raleigh was the first pioneer to use piezoelectricity but the first through investigation was by Jacques and Pierre Curie in 1880 [49]. The heart of the QCM is the piezoelectric quartz crystal sandwiched between a pair of electrodes as shown in Fig. 9. There is cut-angle with eigenfrequencies ranging from $5\times10^{2}$ to

$3\times10^{8}$ Hz. A quartz crystal microbalance is a shear mode device in which the acoustic wave propagates in a direction perpendicular to the crystal surface [50]. A piezoelectric quartz crystal is a precisely cut slab from a natural or synthetic crystal of quartz. The quartz crystal plate must be cut to a specific orientation with respect to the crystal axes. These cuts are $X$ -cut, $Y$ -cut, $AT$ -cut and $BT$ -cut. $AT$ –cut crystals are most useful as piezoelectric immunosensor. The application of an external electrical potential to a piezoelectric material produces internal mechanical stress. A QCM is a shear mode device in which the acoustic wave propagates in a direction perpendicular to the crystal surface. Andreas Janshoff *et al* explained thickness-shear-mode (TSM) resonators in QCM made form $AT$ -cut crystals by cutting angle at $35.25^{o}$ to the $Z$ -axis, platform and high frequency stability of $^{o}C$ . Since $AT$ -cut quartz crystals have a temperature coefficient that is almost zero between 0-50 $^{o}C$ , this particular cut is the most suitable one for QCM sensors. Crystal is coated with gold on both sides because gold is not oxidizing like silver. The understanding of this mass induced frequency shift is only known on a qualitative basic. In 1959 Sauerbrey, the physicist of Germany discussed the frequency shift of a quartz crystal resonator that is directly proportional to the added mass. Sauerbreys work was generally taken as the breakthrough and the first step toworded a new quantitative tool to measure very small masses [51-58].

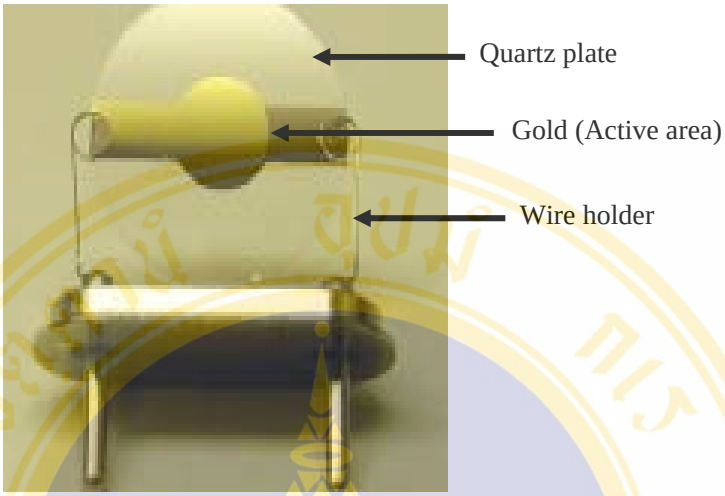


**Figure 2.3** Piezoelectric quartz crystal microbalance

If a rigid layer is deposited on one side or both sides of the electrodes, the resonant frequency will decrease proportionally to mass on the crystal according to Sauerbrey equation:

$$\Delta f = -2.3\times10^{-6} f_0^2 \Delta m/A \qquad (1)$$

where $\Delta f$ is measured frequency shift; $f_0$ is resonant frequency of the fundamental mode of the crystal; $\Delta m$ is the mass change per unit area $AT\ g/cm^2$; $A$ is piezoelectrically active area ($cm^2$).

Sauerbrey equation could be only applicable to uniform, rigid, thin-film deposits. If the thickness of crystal is too thin (less than $500^o A$) the resonant frequencies of regions with and without electrode are very similar, therefore the acoustic wave is not confined to the electrode-covered region, and as a consequence the quality factor $Q$ of the resonator decrease. Thick electrodes cause a decrease in the $Q$-factor as a result of the presence of a dead dielectric, which is particularly pronounced by using gold

electrodes and high frequency resonators. Sauerbray equation does not apply for thick film, viscous liquids, elastic solids, and viscoelastic bodies. Therefore, the development of special oscillator circuits was necessary to cope with the high damping with liquid loads. Until the beginning of 1980's scientists realized that a quartz crystal could be excited to a stable oscillation when it was immersed in a liquid. Kanazawa *et al* were pioneer in liquid phase QCM measurements. They showed that the change in resonant frequency of a QCM taken from air into a liquid is proportional to the square root of the liquid's density-viscosity product [59]:

$$\Delta f = -f_u^{3/2}\left[\left(\rho_L \eta_L\right)/\left(\pi \times \left(\rho_q \mu_q\right)\right)\right]^{1/2} \qquad (2)$$

where $\Delta f$ is measured frequency shift; $f_u$ is the resonant frequency of the unloaded crystal; $\rho_L$ is the density of liquid in contact with the crystal; $\eta_L$ is viscosity of liquid in contact with the crystal; $\rho_q$ is density of quartz; $\mu_q$ is shear modulus of quartz.

An excessive viscous loading would not prohibit use of the QCM in liquid. Response of the QCM is still extremely sensitive to mass changes at the solid-liquid QCM.

As the coating layer becomes complex, however, additional physical factors need to be involved to describe the characteristic of sensor response. Figure 2.4 represents a side cross-sectional view of a QCM in thickness shear mode and with a selective layer, an antibody film here, attached on it. $h_q$ and $h_f$ are the thickness of the quartz plate and the film respectively. In case of a QCM immunosensor coated with antibody layer and/or other biomolecules, the profile of the sensor response does not always follow the equation (1) or (2). To examine more detailed behavior of the frequency responses in this particular situation, we review the partial differential equation for the frequency shift of QCM based sensors developed by Hunt *et al* [60] from the complex reciprocity relation and time-dependent perturbation theory.

$$t\frac{\partial \Delta\omega}{\partial t} + \Delta\omega = \frac{\omega_u h_f}{\pi\sqrt{\rho_q \mu_q}}\left\{-\omega_u\left[\Delta\rho - \frac{\Delta\mu}{V_s^2}\right] + j\left[\frac{\partial \Delta\rho}{\partial t} - \frac{1}{V_s^2}\bullet\frac{\partial \Delta\mu}{\partial t}\right]\right\} \qquad (3)$$

where $V_s$ is the acoustic velocity across the thickness; $\rho$ is the density of the film; $\mu$ is the stiffness ($N/m^2$) of the film; $\Delta$ is the difference between perturbed and unperturbed quantities.

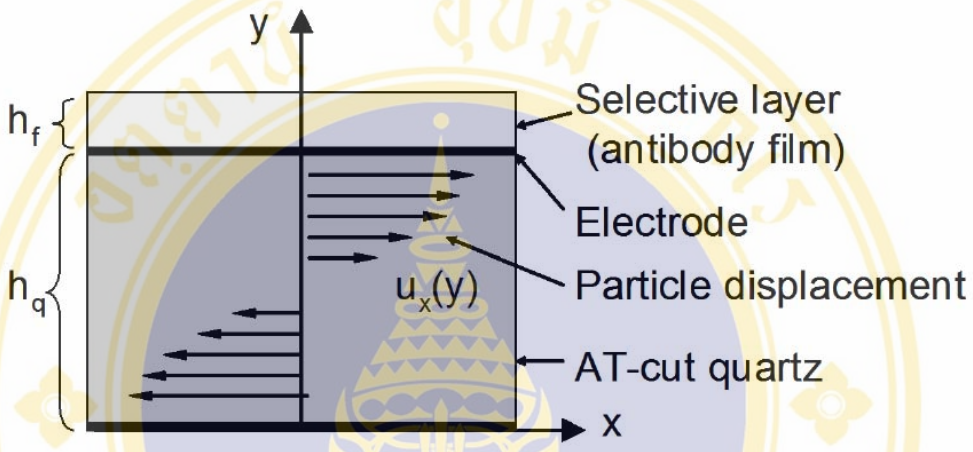


**Figure 2.4** Side cross-sectional diagram of a QCM with biofilm coated

Assuming that neither $\Delta\omega$, $\Delta\rho$, or $\Delta\mu$ changes with time, we get

$$\Delta f = -\frac{2 f_u^2 h_f}{\sqrt{\rho_q \mu_q}}\left[\Delta\rho - \frac{\Delta\mu}{V_s^2}\right] \quad (4)$$

Noting that $\mu_q$ and $\rho_q$ are constants the mass loading can be expressed as $m = \rho A h_f$, equation (4) is essentially the Sauerbrey equation (1) with an additional term describing changes in the mechanical stiffness of the film. This equation predicts that mass loading will lower the frequency but increase in stiffness will incur a positive frequency shift. Note that neither (1) nor (2) can explain a positive frequency shift. If $\Delta\rho$ and $\Delta\mu$ were known as function of time, the solution would be

$$\Delta\omega(t)=\frac{1}{t}\left(\int_t \frac{\omega_u h_f}{\pi\sqrt{\rho_q\mu_q}}\left\{-\omega_u\left[\Delta\rho(\tau)-\frac{\Delta\mu(\tau)}{V_s^2}\right]\right\}d\tau + j\left[\Delta\rho(t)-\frac{\Delta\mu(t)}{V_s^2}\right]+C\right) \qquad (5)$$

Though $\Delta\rho$ can be extracted from kinetic approximations, $\Delta\mu$ is a complete unknown. This equation represents a mathematical tool for extract conformational change data from real-time QCM measurements by recording $\Delta\omega_t$ .

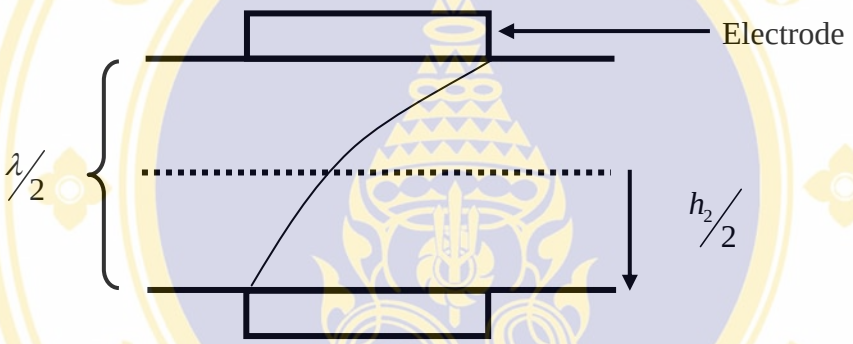


**Figure 2.5** Cross sectional view of quartz crystal microbalance showing reflected thickness shear wave, $h_s$ is the thickness of the crystal and $\lambda$ is the wavelength

### 2.1.3 Measuring system

Measuring system of piezoelectric biosensor consists of oscillator circuit and frequency counter as shown in Fig. 2.6. The piezoelectric quartz crystal sensor utilizes oscillation to detect and identify the mass of bacteria from intrinsic oscillator. The oscillation is converted into pulses by oscillator circuit. The number of the pulses is counted by a frequency counter. Currently the piezoelectric crystal has basic resonant frequency between 10-30 MHz. Higher frequencies are not routinely used as

the quartz plates become too thin and fragile. Effects influence to oscillation frequency such as the thickness, density, shear modulus of the quartz, and the physical parameters of the adjacent media (density or viscosity of air or liquid).

In 1991 Shakal *et al* showed the suitable oscillator circuit 10 MHz. from Texas Instruments. Oscillator circuit driving the crystal provided enough energy to the crystal's vibration. The simple construction was based on the gate oscillator as shown in Fig. 2.7. Better stability is obtained using carefully designed lever oscillators consisting of individual transistors. CMOS-IC's in crystal oscillators is quit popular [24].

Shu-Fen Chou *et al* proposed an oscillators circuit builted in-house to amplify the signal of resonant frequency of the oscillator as shown in the Fig.2.8. They used crystal 10 MHz. for determining of alpha-fetoprotein (AFP) in human serum. Their oscillator circuit supported the measuring system of AFP concentration from 0.1-100 µg/L successfully [30].

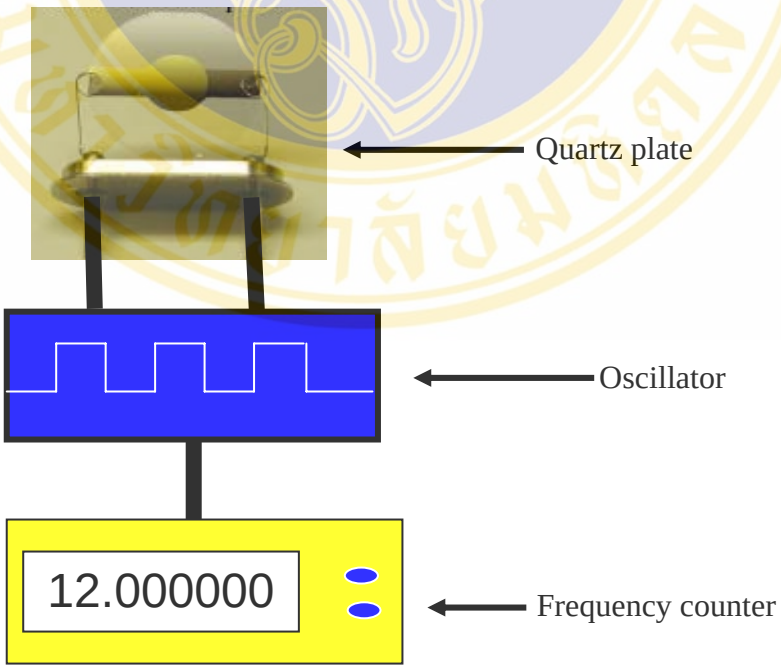


**Figure 2.6** Measuring system of piezoelectric biosensor consists of quartz plate, oscillator, and frequency counter

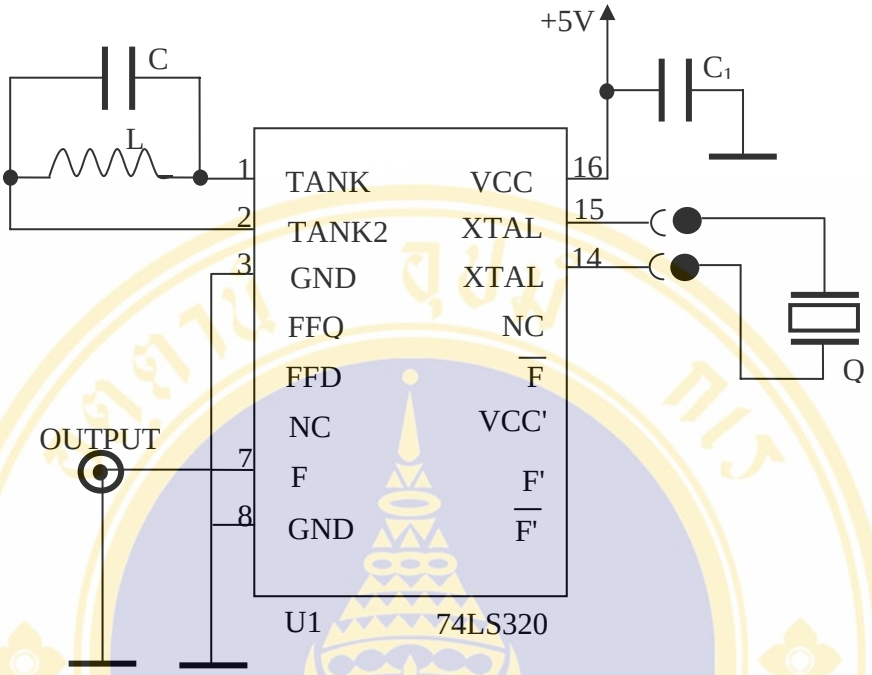


**Figure 2.7** Oscillating circuit of Skaldal (74LS320) [24]

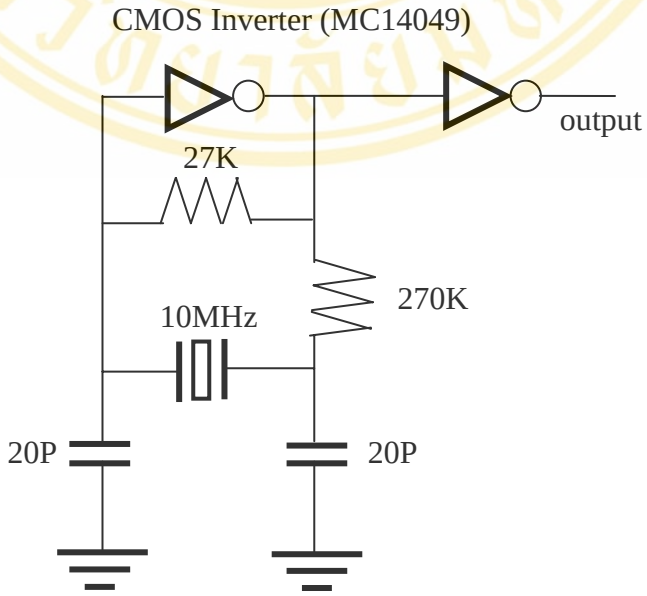


**Figure 2.8** Oscillating circuit by CMOS inverter (MC14049) [30]

Andreas Janshoff *et al* studied the binding of bacterial toxin with ganglioside containing solid supported membranes. The ability of the gangliosides to act as suitable receptors for the different toxins was tested by measuring the changes of quartz resonance frequencies. Their oscillator circuit consisted of an integrated circuit SN 74 LS 124N from Texas Instruments and an oscilloscope in order to control the oscillation. They could detect frequency shift within the range of 28-99 Hz [48].

Reza Saber *et al* exposed their oscillator circuit, a typical Colpits oscillator, which has a buffer amplifier. Fifteen DC volts were applied to the oscillator circuit to drive the crystal. Colpits oscillator is a part of human serum albumin (HSA) detection in aqueous media. An increase in frequency shifts was observed during increasing of HAS concentration of 16-128 µg/ml. Flow system effected crystal's oscillation. Many rollers in flow system produced pulsatile noise [61-65]. Most of scientists constructed simple oscillator circuit but they used commercial frequency counter, for example, Hewlett-Packard frequency counter (Model No: HP 53181 A, 225 MHz.) [60].

Hidenobu Aizawa *et al* invented immunosensor for C-reactive protein (CRP) detection. CRP is one marker protein which is increased in quantity during acute inflammation or tissue damage especially pneumonic in the elder. This equipment covered the concentration range required to determine the amount of CRP less than 1 mg/dl in blood sample. A prototype of a portable CRP sensor system could be operated with either batteries or an AC adaptor. A commercially available frequency counter kit and a lab–made oscillation circuit in contact with the solution were integrated into this sensor system. CRP sensor is shown in Fig.14 [66].

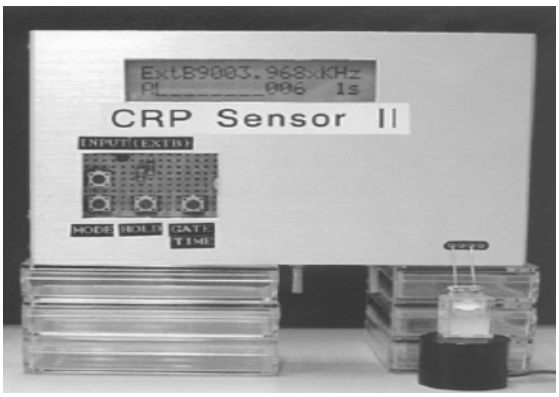


**Figure 2.9** Photograph of the experimental setup of CRP Sensor II [66]

## 2.2 Improvement Biological Phase

This phase consists of the two important parts; immobilization of antibodies presented in 2.2.1 and evaluation of affinity interaction displayed in 2.2.2, respectively.

### 2.2.1 Antibody immobilization

The secondary phase presents the immobilization of antibodies on gold disk surface, primarily. Immobilization is the process of attaching biological components to the transducer which can be separated into five methods [67].

**1) Adsorption** is the simplest and minimal preparation, but molecule attachment is weak. Adsorption has two types: Physical and chemical adsorption. Physical adsorption is the weak bond via the formation of Van der Waals, occasionally with hydrogen bonds or change-transfer forces. Chemical adsorption is much stronger and attaches with covalent bonds [68-72].

The most model equations used is the Langmuir adsorption isotherm.

$$\theta = K\rho_a /(1+K\rho_a) \tag{6}$$

where $\theta$ = the fraction of the surface covered

$\rho_a$ = pressure of adsorbent

$K$ = $K_a/K_d$ ; $K_a$ = rate constant for adsorption,

$K_d$ = rate constant for desertion

Adsorption method senses to change in pH, temperature, ionic strength and the substrate. However, this technique is only suitable for exploratory work over a short time-span [73-75].

**2) Microencapsulation** uses biomaterial helping in place behind a membrane for closely contacting between the biomaterial and the transducer. This method is no interfering with the reliability of the enzyme. Causations have the contamination and biodegradation of biomolecules. However, microencapsulation is stable to changes in temperature, pH, ionic strength and chemical composition. Inert membrane is used to trap the biomaterial on the transducer. This technique has many advantages; to be closely attachment between the biomaterial and the transducer, to be very adaptable, and to be very reliable specific to biomaterial e.g. high specificity and good stability to change in temperature, pH, ionic strength, and substrate concentration. Some examples of microencapsulation are polycarbonate (Nuclepore) PTFE (polytetrafluoroethylene or Teflon)

**3) Entrapment** is the technique by mixing between biomaterial and monomer solution, then mixer solution is polymerized to a gel, trapping the biomaterial. The most used gel is polyacrylamide, starch gels, nylon, silastic gels, and polypyrrole. Unfortunately, this can cause barrier to the diffusion of substrate, thus slowing the reaction and then slow response time of biosensor. Moreover, activity of enzyme may be dropped when it is trapping through the pores in the gel.

**4) Cross-linking** is the attachment, which is chemical bond to solid supports or to another support such as gel e.g. glutaraldehyde. This method limits diffusion and may be damage biomaterial and mechanical strength is poor, but stabilizes absorbed biomaterials. It is useful method to stabilize absorbed enzyme. However, this technique causes damage to the enzyme, limits diffusion of the substrate and poor rigidity (mechanical strength). e.g. 1,5-dinitro-2-4-difluorobenzene [76-80].

**5) Covalent bonding** consists of some functional groups, such as $NH_2$, $CO_2H$, $OH$, $C_6H_4OH$, $SH$ and imidazole, which no reach with catalytic activity of an enzyme can be covalently bonded to the support matrix (transducer or member). This bonding type is suitable during using because enzyme or biomolecules will not release and protect the active site of biomolecules. Nevertheless, this type of bond should be

under mild conditions, for example low temperature, low ionic strength and pH in the physiological range [81-86].

**The lifetime of the biosensor is enhanced by proper immobilization**

| | | |
|---|---|---|
| Absorption | 1 | day |
| Membrane entrapment | 1 | week |
| Physical entrapment | 3-4 | weeks |
| Covalent entrapment | 4-14 | months |

Every bond can amount to changing the structure of the electrode material at the surface or to coating the surface with a new material which can have a highly specificity, sensitivity, and reproducibility of biosensors.

This experiment emphasizes at adsorption technique because it is suitable to study initially, save cost, and facilitate to work in the laboratory. Physical adsorption is a type of immobilization techniques that is routinely used for antibody and receptors. This method is relatively simple and has been shown to be satisfactory for a limited number of assays using the same sensor (usually only single use for physical adsorption immobilization). Most using protein A (SpA) is produced from *Staphylococcus aureus*, gram positive bacteria. Protein A binds to $F_c$ part of antibodies with specifically, therefore $F_{ab}$ region of antibodies properly orients bind to epitope of antigen.

The immobilization technique of antibodies leads to an accuracy fundamental frequency ( $f_0$ ) on QCM surface. It determines the sensitivity of the biosensor. Immunologists desire the chemical compound to function as connector between $F_c$ of antibodies and gold surface as shown in Fig. 2.10. $F_{ab}$ domain of antibodies will bind with bacteria antigen. Immunosensors can increase specificity by using monoclonal antibodies which specify only one type of bacteria species.

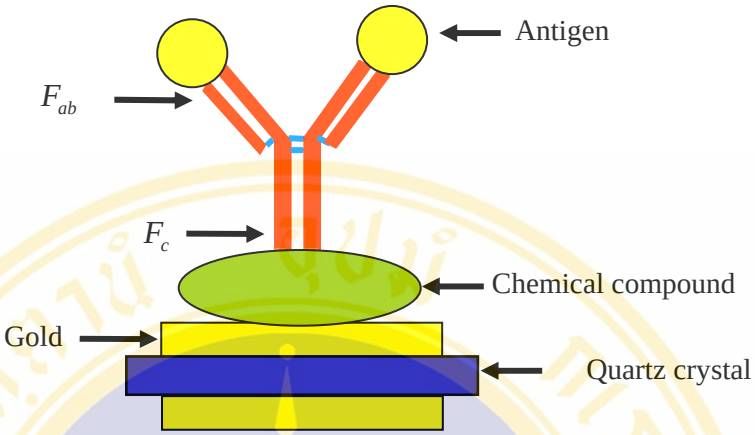


**Figure 2.10** Chemical compound coated on crystal surface

Kurosawa *et al* discussed that the popular methods had many techniques such as physical adsorption, Protein A, Cystaminine-glutaraldehyde, Cystamine, Con A, and Latex method [87].

In-seon Park *et al* improved coating method by using thiolate group. This immobilization method exploited a direct covalent bond formation between one gold electrode of a quartz crystal surface and a thiolated antibody raised against the common structural antigen of *Salmonella* spp. A thiolate reagent worked as a cleavable cross-linker, introducing available sulfhydryl groups to an antibody. A monolayer coating of the thiolated antibody onto the gold surface was easily done by covalent bond formation because the reaction potential between the gold and sulfur was very strong. 6-[3-(2-pyridyldithio)propionamido]hexanate(sulfo-LC-SPDP(sulfo-LC-SPDP) thiolation was the best chemical reagent for coating the antibody onto the crystal considering sensitivity and stability obtains. They used anti-*Salmonella* antibody 0.5 mg/ml. This sensor could detect the *Salmonella* spp. ranging from $9.9\times10^{5}$ to $1.8\times10^{8}$ CFU/ml [29].

Reza *et al* [61] developed an immunoaffinity sensor for human serum albumin (HSA). Anti-HAS antibodies were immobilized via these amino groups by using

glutaraldehyde (GA) as cross-liker. An increase for the frequency shifts was observed with increasing of HAS concentration of 16-128 µg/ml [60].

Ashok Kumar described crystal electrodes were coating of protein A for better adhesion of the antibodies to the crystal surface. Protein A entrapped antibodies on the crystal surface. Protein A was a polypeptide isolated from *Staphylococcus aureus* that bound specifically to the immunoglobulin molecules, especially immunoglobulin G (IgG) antibodies, without interacting at the antigen site. This property permitted the formation of tertiary complexes consisting of protein A, antibody and antigen. His objective detected mycobacterial antigens in diluted cultures of *Mycobacterium Tuberculosis* which causes tuberculosis (TB) [31].

Hua Wang could detect *Toxoplasma gondii*, caused Toxoplasmosis, by attaching anti-*Toxoplasma gondii*. Toxoplasmosis is the ubiquitous disease generally asymptomatic in immunocompetent hosts, whereas leads to optical, neural and visceral damages. He used plasma-polymerized film (PPF) of n-butyl amine and heparin layer for preparing material of probe. His experiment gets result in a response-enhanced immunoagglutination and a high compatibility of the probe. He reported the sensitivity to dilution ratio of anti-*T. gondii* as low as 1:5500 [61].

Shu-Fen Chou *et al* presented that self-assembled monolayer prepared by the cystamine method (chemical bonding) for detecting alpha-fetoprotein (AFP) in human serum. Hepatocellular carcinoma and teratoblastoma disease found the high level of AFP in patients' serum. Their technique could detect AFP concentration from 0.1 to 100 µg/ml. Moreover, they reported that frequency shift were all over 95% of those on the response at the first day when they reproduce these immunosensors [30].

In 2006, M.lazerges *et al* detected Alexandrium minutum DNA, a microalgae that produces neurotoxins responsible for paralytic shellfish poisoning on European and Asian coasts. He immobilized 20-base DNA (single stand DNA) and its result to 47% hybridization ratio for a coating sequence of Alexandrium minutum DNA. This method could reproducible up to 4 times in the measurement of this type of DNA [88].

Xiao-Li Su and Yanbin Li applied protein A for the antibody immobilization in diagnosis of *Salmonella Typhimurium*. Frequency shift could be detected in the range from $10^5$ to $10^8$ cells/ml in suspension of bacteria concentration. Continually, they

utilized anti-*Salmonella*-magnetic beads for signal amplification, but frequency shift was not related to the cell concentration [89].

A major problem of immobilization remains the nonspecific adsorption at the QCM surface; hence the sensitive area is blocked with a protein such as Bovine serum albumin (BSA) or casein before the binding of the bacteria antigen to minimize nonspecific adsorption. Reusability of QCM is important criteria in choosing immobilization techniques because of saving money. Most recently, novel immobilization methods, in terms of self-assembled monolayer (SAM), have been developed in QCM modification. SAM techniques result in orientation immobilization of antibodies. A surfaces fabricated method called SAM can withstand more cycles of regeneration.

Xia Chu *et al* introduced the new amplify signal method, a novel dendritic amplification procedure. The first antibodies were immobilized on the quartz crystal surface with using protein A adsorption. Then antigen in the solution recognized with first antibody to occur the antigen-antibody complex (Direct immunoassay). Antibodies-functionalized gold nanoparticles are a small particle which was surrounded with secondary antibodies. This technique can help to amplify signal to detect clearly [90].

### 2.2.2 Evaluation of affinity interaction

This part is the evaluation of affinity interaction. Hepel studied of affinity interaction especially kinetic rate constants in 1999. The piezosensors are suitable for kinetic characterization of affinity binding reactions to measure concentration and combine of electrochemical reaction [30]. Antigen-antibody complex causes mass change on the crystal surface. Formation of this complex presents the kinetic association $K_a$ and dissociation $K_d$ rate constants as shown in Fig. 16.

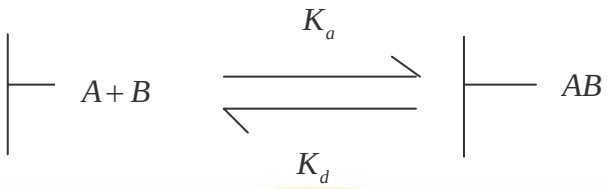


**Figure 2.11** Formation of the antigen-antibody complex. $A$ is the antibody; $B$ is the antigen or analyte; $AB$ is the antigen-antibody complex [91]

At equilibrium point, the equilibrium constant ($K$) depends on the direction of the equilibrium that can separate two parts, $K_a$ (an association equilibrium constant) and $K_d$ (a dissociation equilibrium constant).

$$K_a = \frac{[AB]}{[A][B]} \tag{7}$$

$$K_d = \frac{[A][B]}{[AB]} \tag{8}$$

The equilibrium is a dynamic situation, therefore complex formation and dissociation continuously occurs. The $K$ does not constant because of time required to reach equilibrium.

**Association:** $A + B \rightarrow AB$

$$d[AB]/d[t] = k_d[A][B] \quad (9)$$

**Dissociation:** $AB \rightarrow A + B$

$$d[AB]/d[t] = k_d[A][B] - k_d[AB] \quad (10)$$

where $k_d$ ($s^{-1}$) is the dissociation rate constant, which indicates the $AB$ complex dissociated per second.

Using fm as the frequency change after a complete situation of the surface of the crystal with antibodies, the concentration of the free antigen $B$, $[B]$, is proportional to $(f_m - f)$ and the concentration of the complex $AB$, $[AB]$, to $f$.

This equation can thus be expressed as:

$$Df/dt = k_a C(f_m - f) - k_d f \quad (11)$$

where $C$ is the concentration of the free antibody $A$.

Antigen-antibody complex (Ag-Ab complex) is the non-linear regression [Figure 2.12] of piezoelectric immunosensors. $f_0$ is a stable background signal. Injection of analytes goes to the immunusensor after that analytes combine with antibodies. Ag-Ab complex increases mass on QCM decreasing the resonant frequency until the equilibrium point; resonant frequency change goes to constant frequency ($f_{eq}$). $f_0$ represents the amount of the surface-bound immunocomplex at the beginning of the dissociation [15].

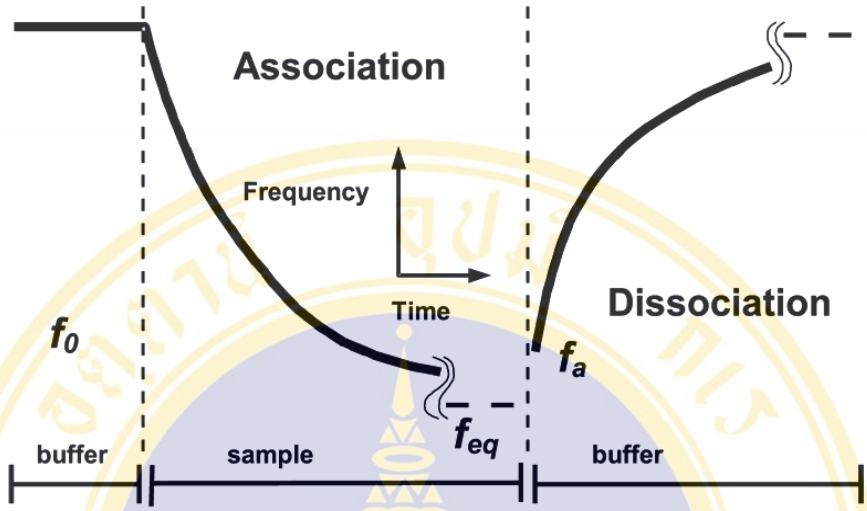


**Figure 2.12** Characterization of kinetic properties of antibodies. First, the background signal is recorded in the carrier buffer only, association reaction in the presence of the sample follows-formation of immunocomplexes at the sensing surface and finally spontaneous dissociation of immunocomplexes is observed in the absence of the sample [31]

In 2005, Sang-Hun Lee *et al* found that high flow rate would result in the analytes being swept out without having a chance to bind to antibodies [38]. If too low a flow rate would incur unnecessary accumulation of unbound analytes near the sensor surface, which hinders the binding events. Of course, the choice of optimal flow rate depended on the structure of a flowcell and the size of inject-tube. Therefore, evaluation of affinity interaction between antigen and antibody is based on purification of antibody, immobilization of antigen on QCM and creation a flow system [92].

From Literature review, piezoelectric immunosensors have many advantages in various fields especially clinical diagnosis. Food contamination by *v. cholerae* O1 toxins is one of the most serious concerns today. Hence there is a critical need for a rapid and reliable analytical method for detecting these microorganisms. Conventional

microbiological culture methods are uncomfortable and time-consuming. Recently, the specificity of antibody-antigen reaction has been utilized in immunosensors making use of piezoelectric crystal. This thesis chooses *AT*-cut crystal coated with gold electrode on both sides because *AT*-cut crystal is more suitable in quartz immunosensors than other crystals from published report of Anreas Janshoff in 2002 [93]. Polyclonal antibodies are immobilized on the crystal surface with protein A. The availability of monoclonal antibodies specifies to single bacteria species (recognizing particular epitopes of bacteria). The polyclonal anti-*V. cholerae* O1 antibodies do not cross reaction with other vibrio types; therefore piezoelectric immunosensor is highly sensitive and specific. Antigen-Antibody complexes load on the crystal surface since quartz crystal oscillation decreases from prior frequency. Frequency shift can be measured by frequency counter adapted from PIC microcontroller. There is highly possible opportunity for construction of *v. cholerae* O1 sensor based on piezoelectric quartz crystal microbalance.

# CHAPTER III
# METHODOLOGY

This chapter focuses on the separate materials and methods used in this research. Materials consist of chemical reagents and electronic hardware. Subsequently, method illustrates the research process in chronological fashion.

## 3.1 Materials

### 3.1.1 Reagents and Microorganism

Chemicals used in this study were analytical and molecular biological grades

**Reagents:**

| Chemical name | Molecular Weight | Company |
|---|---|---|
| Absolute ethanol | 46.07 | E. Merck |
| Hydrochloric acid, HCl | 36.5 | E. Merck |
| Sodium chloride, NaCl | 58.44 | BDH |
| Sodium hydroxide, NaOH | 40 | Sigma |
| Bovine serum albumin, BSA | - | Sigma |
| Protein A | 45,000 | Sigma |
| 30% Hydrogen peroxide, $H_2O_2$ | 34.1 | MERCK |
| Sodium phosphate monobasic, $KH_2PO_4$ | 136.1 | Sigma |
| Sodium phosphate dibasic, $Na_2HPO_4$ | 142 | Sigma |
| | | |

**Microorganism:**

- *Vibrio cholerae* O1
- Polyclonal anti-*V. cholerae* $O_1$

### 3.1.2 Instruments

| Instrument name | Company | Country |
|---|---|---|
| Desiccator | Nikko | Japan |
| Incubator | Termarks | Norway |
| Staftech Fume Hood | Staftech CO., LTD | Thailand |
| Mini Rocker MR-1 | Biosan | Germany |
| Computer | Hewlett Packard | USA |
| Frequency counter | Good will instrument CO., LTD | Taiwan |
| WINPIC800 | Innovative Experiment | Thailand |
| Water bath | PolyScience | USA |
| Ultrasonic | J.P.SELECTRA | Spain |
| Staftech Fume Hood | Staftech CO., LTD | Thailand |
| Precisa XT 2200C | Precisa Instruments, LTD | Switzerland |

### 3.1.3 Laboratory Equipments

- An AT-cut piezoelectric quartz wafer 12 MHz, 6 mm X 6 mm X 100 Angstroms
- Pierce oscillator, SN 74 HC245; CMOS inverter of Texas Instruments Inc.
- PIC18F458 microcontroller, Microchip Inc.
- MPLAB
- Automatic pipettes; 20-1000 µl, Eppendrof Inc., Hamburg, Germany

### 3.1.4 Sample for Bacterial Extraction

The organisms used in this study were from the Department of Clinical Microbiology, Faculty of Medical Technology, Mahidol University, Thailand. They were identified by biochemical testing and verified with according to the standard protocol for bacterial identification as a gold standard.

### 3.1.5 Preparation of Reagents

#### 3.1.5.1 Agar

In order to prepare the agar, 23.4g of agar powder was suspended in 1 L of purified water, mixed thoroughly by stirring and heated for 1 min to completely dissolve the powder. This was finally autoclaved at 121$^{o}C$ for 15 min.

#### 3.1.5.2 10x Phosphate Buffer Saline (PBS), pH 7.4

The solution of 10x PBS pH 7.4 was prepared by dissolving 80g of Sodium Chloride, 2g of Potassium chloride, 11.5g of Sodium Phosphate, Dibasic, Heptahydrate ($NaHPO_4 7H_2O$), and 2g of Potassium dihydrogenphosphate ($KH_2HPO_4$) in 1L of distilled water. This solution was also autoclaved at 15 psi for 30 min and then kept at room temperature.

#### 3.1.5.3 1x Phosphate Buffer Saline (PBS), pH 7.4

One volume of 10xPBS was added to 9 volumes of distilled water and then autoclaved at 15 psi for 30 min. This solution was kept at room temperature.

#### 3.1.5.4 1% Bovine Serum Albumin (BSA) Solution

One mg of Bovine Serum Albumin powder was dissolved in 100 ml of distilled water. This solution can be kept at 4$^{o}C$ for one week.

#### 3.1.5.5 0.8% Sodium Chloride (NaCl) Solution

The solution was prepared by dissolving 0.8mg of Sodium chloride powder in 100ml of distilled water and sterilized by autoclave at 15 psi for 30 min. This solution was kept at room temperature.

#### 3.1.5.6 Piranha Solution

One volume of Hydrogen peroxide ($H_2O_2$) was added to 3 volumes of conc. Hydro sulfuric acid ($H_2SO_4$). This solution was kept at room temperature.

## 3.2 Methods

This study is composed of two important phases; the development of an electrical phase and biological phase. In the first phase, the development of the electronic phase, an electronic circuit was built to the piezoelectric crystal with *AT* -cut quartz wafers that have characteristic resonant properties of Sauerbrey equation. Fromm Sauerbrey equation, the relationship between mass of an adsorbed rigid film and the resonant frequency changes: The change of the resonant frequency of the piezoelectric crystal is thus directly proportional to the mass change on quartz crystal surface. A pic-microcontroller, a frequency counter, was developed and used with an oscillator which measures frequency shift on the quartz surface when absorption of biomolecules attached at this area are absorbed. The development of biological phase, the second phase, presented the immobilization method of an anti-*V. cholerae* O1 as a capture antibody. These antibodies were specific to *v. cholerae* O1 antigen.

### 3.2.1 Electronic Development Phase

An AT-cut piezoelectric quartz wafer, diameter of 6 mm was placed between two gold electrodes. The resulting crystal has a fundamental resonant frequency of 10 MHz. It was mounted in a dip holder with a plug and was connected with an oscillator module (Pierce oscillator, SN 74 HC04) as shown in Fig. 3.1. The recommended frequency range of a pierce oscillator is between 100 kHz to 20 MHz, as its relative frequency stability is high and waveform is good when its frequency is

above 3 MHz [33]. Subsequently, a PIC18F458 microcontroller functioned as a quartz crystal analyzer for detecting the frequency shift. Figure 3.2 shows the piezoelectric immunosensor which was built from an elementary PIC-microcontroller and an oscillator circuit. The quartz crystal analyzer system was connected to LCD (Liquid Crystal Display) in order to monitor the frequency shift.

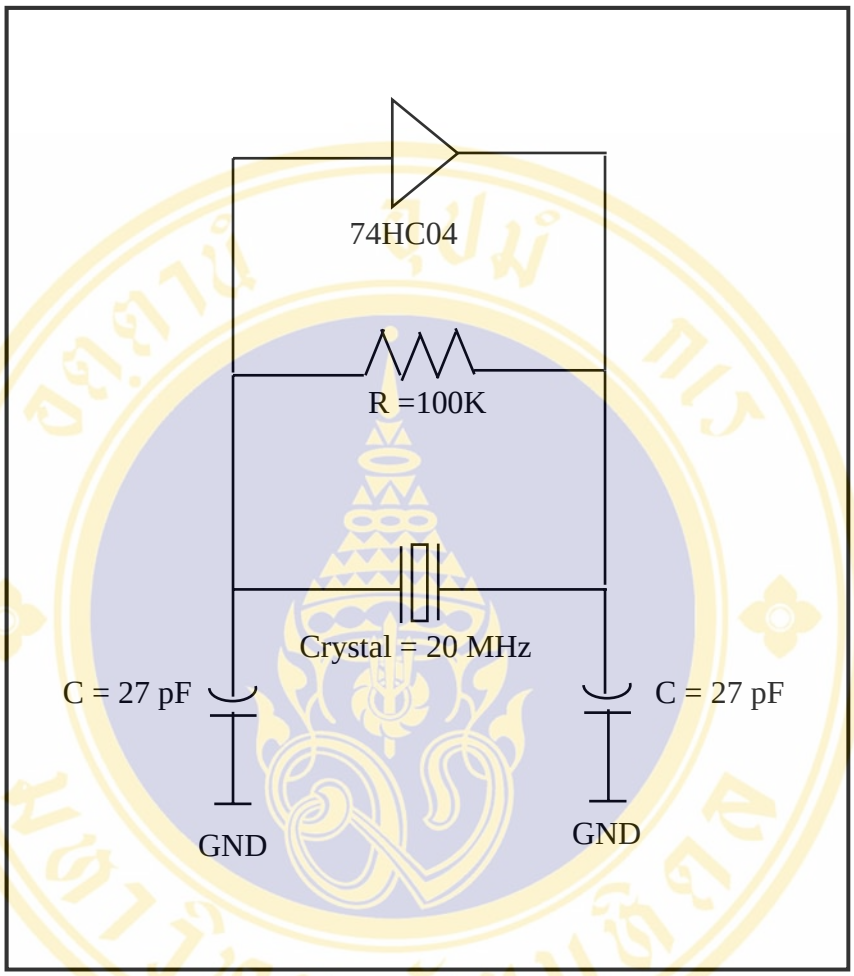


**Figure 3.1** Pierce crystal oscillator: schematic diagram. From this diagram, frequency of crystal =12 MHz, R = 100 K, $C_1$ = 27 pF and $C_2$ = 27 pF.

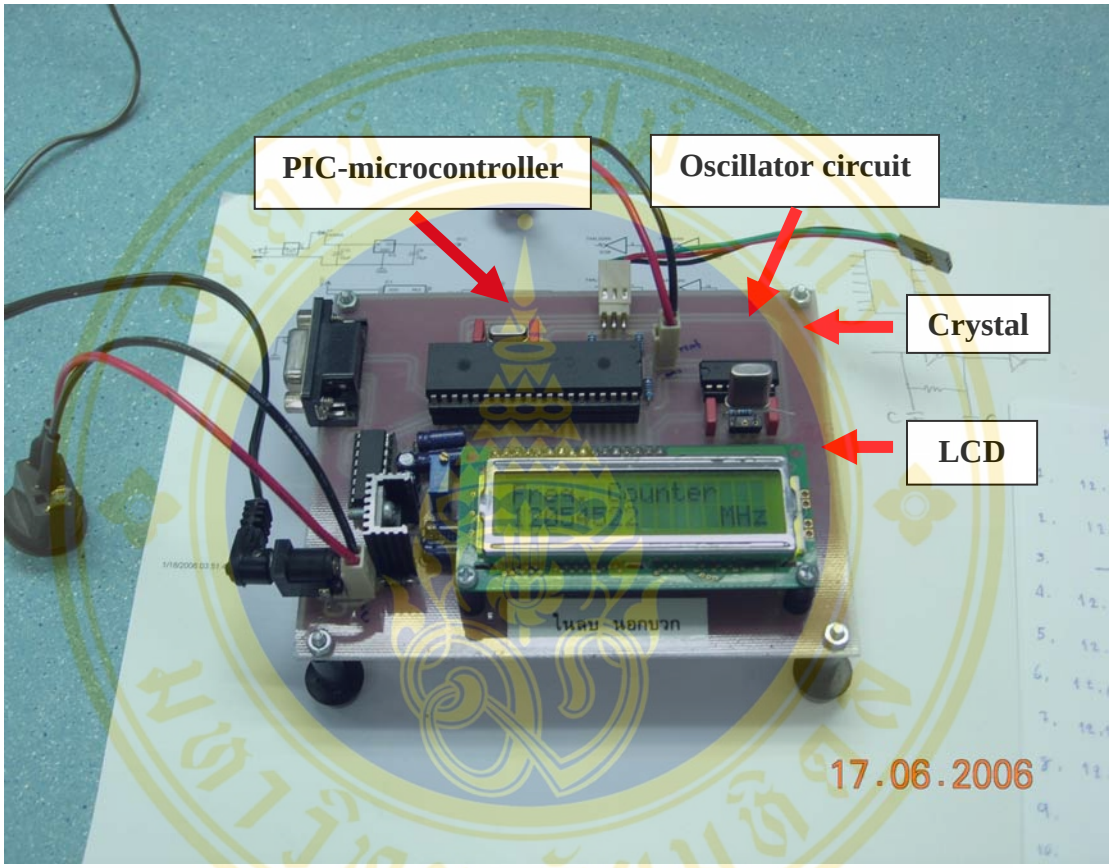


**Figure 3.2** Piezoelectric dry analysis system with a piezoelectric probe for measuring the frequency change of the quartz crystal due to the addition of immobilization layers. The major compositions of the device are composed of PIC-microcontroller, oscillator circuit, crystal and LCD.

### 3.2.2 Biological Development Phase

The biological development phase comprised of studying the optimal detection conditions such as protein A concentration, incubation time of anti- *V. cholerae* O1, or anti-*V. cholerae* O1 concentration, etc. Each optimal condition of these experiments was chosen from the highest frequency shift since the highest point presented the maximum detection of *v. cholerae* O1 antigen attached on the quartz surface. First, to prepare QCM, quartz is cleaned and the fundamental resonant frequency measured. Then, coating of protein A is seen to immobilize the small molecular mass of protein A on the quartz surface, thus the fundamental frequency ( $f_0$ ) was decreased because of a mass deposition of protein A. Next, in order to immobilize the antibody, the crystals that were coated with anti-*V. cholerae* O1 were chemical absorbed. $F_c$ of anti-*V. cholerae* O1 was immobilized by protein A and $F_{ab}$ of these antibodies used the antigen binding site to attach with *v. cholerae* O1 to the specimen. Anti-*V. cholerae* O1 were cross-liked just as in the lock and key theory of immunology. The antibody-coated sensor was dipped into the reaction cell which had a *v. cholerae* O1 suspension of known concentration (CFU/ml) and the frequency shift (Hz) was subsequently measured.

#### 3.2.2.1 Preparation of Quartz Crystal Microbalance

The aim of quartz preparation was to clean the impediments on the quartz surface such as lipid or metal ion to find out the fundamental frequency ( $f_0$ ) with accuracy.

The crystal was soaked in piranha solution for 10 min, washed with distilled water, and dried at ambient temperature for 2 hours. To reduce humidity of the crystal, the crystal was dried for about 1-2 days in the desiccator as shown in Fig. 3.3. The resonant frequency of the crystal was determined until a steady baseline was obtained ( $f_1$ ).


**Figure 3.3** Desiccator used to control humidity on quartz crystal microbalance. It reduces the frequency error from humidity.

### 3.2.2.2 Study the Optimal Detection Condition

The appropriate concentration of protein A and anti-*V. cholerae* O1 was optimized by measurement of specific piezoelectric immunosensor as following:

#### 3.2.2.2.1 Optimization of Protein A Concentration

The concentration of protein A ranging from 0.25, through 0.50, and 0.75, to 1.00 mg/ml were absorbed on the surface of the quartz crystal. The method of coating protein A was showed in Fig. 3.4. The optimal protein A concentration had an important implication: Protein A adjusted $F_{ab}$ of anti-*V. cholerae*

O1 which rotated to attach with *V. cholerae* O1 antigen. Figure 3.5 showed the cause-effect of protein A to bind with antigen. The optimal concentration of protein A, which showed the maximum frequency, was then chosen. These results were reported in Fig. 4.1.

**3.2.2.2.2 Determination of Response *V. cholerae* O1 of Anti-*V. cholerae* O1**

The *v. cholerae* O1 was suspended on one side of a slide while anti-*V. cholerae* O1 was placed on the other side as shown in Fig. 3.6. This experiment was aimed at the anti-*V. cholerae* O1 recognizing the to *v. cholerae* O1 using agglutination technique with optical microscope (100X). Results of agglutination between anti-*V. cholerae* O1 and *v. cholerae* O1 are shown in Fig. 4.2 and compared with an apparatus of with no agglutination normal saline as negative control.

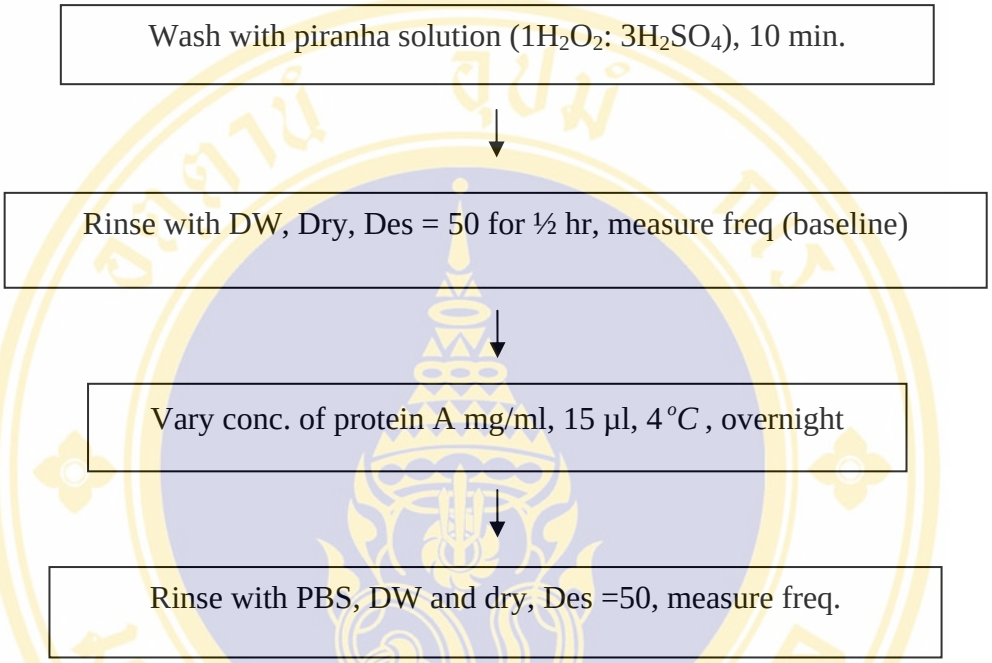


**Figure 3.4** The method of protein A coating. Crystals were cleaned with piranha solution for 10 min, rinsed with distilled water, and dried with air at room temperature (RT). They were brought into desiccator (Des) for a half of hours before measure fundamental frequency of quartz crystal microbalance. Then, coating protein A 15µl followed upon 0.25, 0.50, 0.75, and 1.00 mg/ml, respectively, at 4 $^oC$ , overnight. Next, rinsed with PBS, distilled water and dried with air at RT. They were taken into desiccator and measured the frequency shift (Hz).

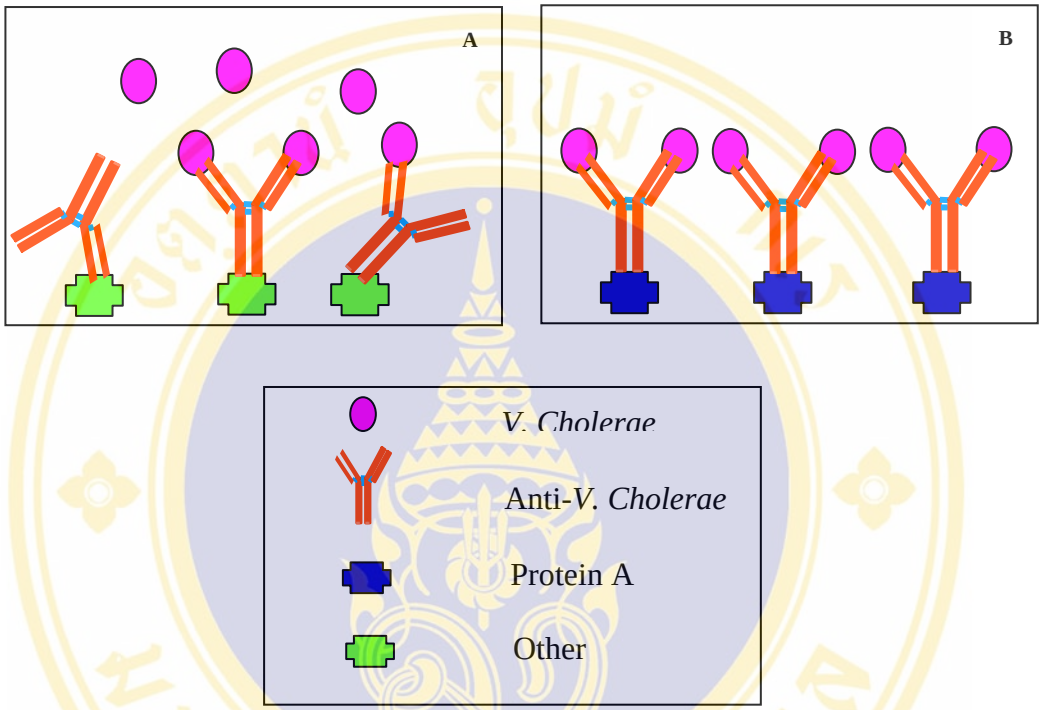


**Figure 3.5** Effecting of protein A to anti-*V. cholerae* O1 immobilization on the quartz surface

**A:** the rotation of anti-*V. cholerae* O1 has several orientations

**B:** molecules of protein A adjust structure of anti-*V cholerae* O1 by linking at $F_c$ part, thus $F_{ab}$ as antigen binding site could attach *v. cholerae* O1 antigen with suitably.

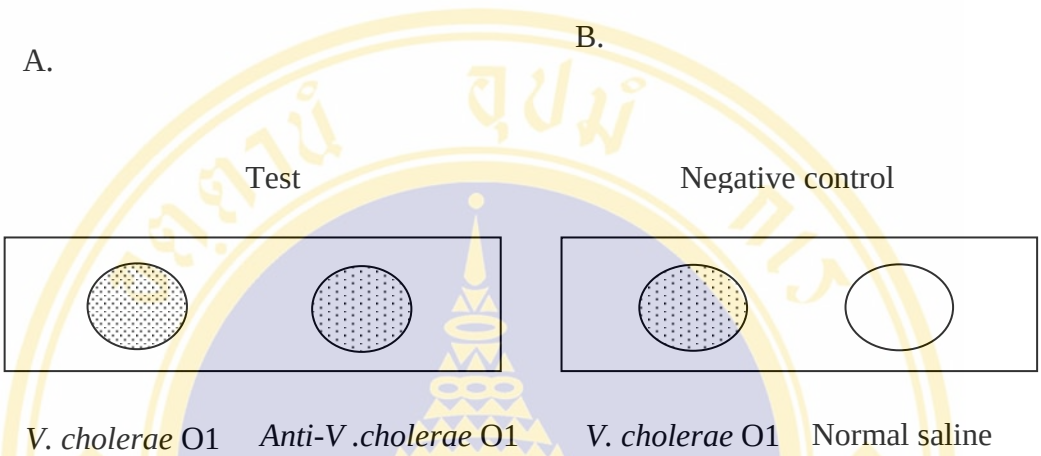


**Figure 3.6** Agglutination of antigen-antibody

***Test slide*;** In the first step, *V. cholerae* O1 and anti-*V. cholerae* O1 is dropped on left and right of the slide in Fig. A.

***Negative control;*** Normal saline is applied on right in Fig B.

Then, test and Negative control are mixed and visualized under a microscopy for determining agglutination of *v. cholerae* O1 and anti-*V. cholerae* O1.

**3.2.2.2.3 Determination of Optimal Incubation Time of Anti-*V. cholerae* O1**

Initially, QCM was cleaned with piranha solution for 10 min and rinsed with distilled water (DW). Then, the QCM moisture was controlled using a desiccator for 30 min before measuring; baseline frequency. QCM was coated with protein A, 1 mg/ml at $4^{o}C$ overnight in a moist chamber. Next, PBS and DW were used to wash out protein A which was not attached to the gold surface. Anti-*V. cholerae* O1, 15 $\mu l$ were immobilized on the quartz surface by incubation time ranging from 0.5, 1, 2, 4, to 8 h. After immobilizing QCM with anti-*V. cholerae* O1, it was dipped into 1%BSA chamber for 1 h at RT. It was again dipped into *v. cholerae* O1 suspension, $10^{8}$ CFU/ml for about 2 h. The QCM was then rinsed with PBS and DW before its humidity was absorbed by a desiccator to measure, final frequency. These results are evident in Fig. 4.3.

**3.2.2.2.4 Study of Binding between Anti- *V. cholerae* O1 and *V. cholerae* O1 by Rotating Method**

The optimum concentration of Protein A, chosen in Fig. 4.1, was applied to this experiment. We applied anti-*V. cholerae* O1 concentration: 0.13 and 0.16 mg/ml by separating two groups. In the first group, anti-*V. cholerae* O1 and *v. cholerae* O1 reaction were rotated with an inverted rotator whereas the second group was not rotated. This experiment was aimed studying whether rotation substantially induced the attachment of the anti-*V. cholerae* O1 at to the *v. cholerae* O1 complex. These results once again are evident in Fig. 44.

**3.2.2.2.5 Optimization of Anti-*V. cholerae* O1**

Finding of the optimal anti-*V. cholerae* O1 concentration was necessary for immobilization of bioimmunosensors because it resulted to the accuracy of these biosensors. The optimal anti-*V. cholerae* O1 concentration immensely assisted in binding *v. cholerae* O1. Figure 3.7 presents anti-*V. cholerae* O1 concentration result to detect *v. cholerae* O1 in specimen.

**Case 1**: Anti-*V. cholerae* O1 concentration had been more over; $F_{ab}$ of anti-*V. cholerae* O1 were more clustered until $F_{ab}$ could not attach itself with *v. cholerae* O1, although a lot of *v. cholerae* O1 antigens remained in the specimen. Frequency shift was lower than real data as shown in 3.7A.

**Case 2**: Anti-*V. cholerae* O1 concentration had been optimal concentration; $F_{ab}$ of anti-*V. cholerae* O1 could attach *v. cholerae* O1, thus frequency shift was more accurate.

**Case 3**: Anti-*V. cholerae* O1 concentration was low; $F_{ab}$ of anti-*V. cholerae* O1 were not enough for *v. cholerae* O1 antigen to signal so detected signal is lower than in case 2. Therefore, frequency shift was of little value.

The first step, the concentration of anti-*V. cholerae* O1 ranging from 0.0750 to 0.2000 mg/ml were absorbed on the surface of the quartz crystal microbalance. Fifteen microliters of various antibody concentrations were spread on the quartz surface for 2 h. Each concentration was immobilized on the quartz and absorbed with the optimum concentration of anti-*V. cholerae* O1. One percent of Bovine Serum Albumin (BSA), which was coated for 1 h, was then used for protecting the non-specific binding from other molecules that could attach themselves to the quartz's surface non-specifically. After immobilizing anti-*V. cholerae* O1, the QCM were immersed into *v. cholerae* O1 suspension, $10^8$ CFU/ml while QCM as inverse-rotated on the rotator. Figure 3.8 is a schematic diagram of the immobilization method of the anti-*V. cholerae* O1 on the quartz surface.

The optimal concentration would present the maximum frequency of QCM. Figure 3.9 displays steps of anti-*V. cholerae* O1 immobilization and the diagram for the immobilization of anti-*V. cholerae* O1, respectively. Results of optimal anti- *V. cholerae* O1 illustrated in Fig. 4.5 and Fig. 4.6.

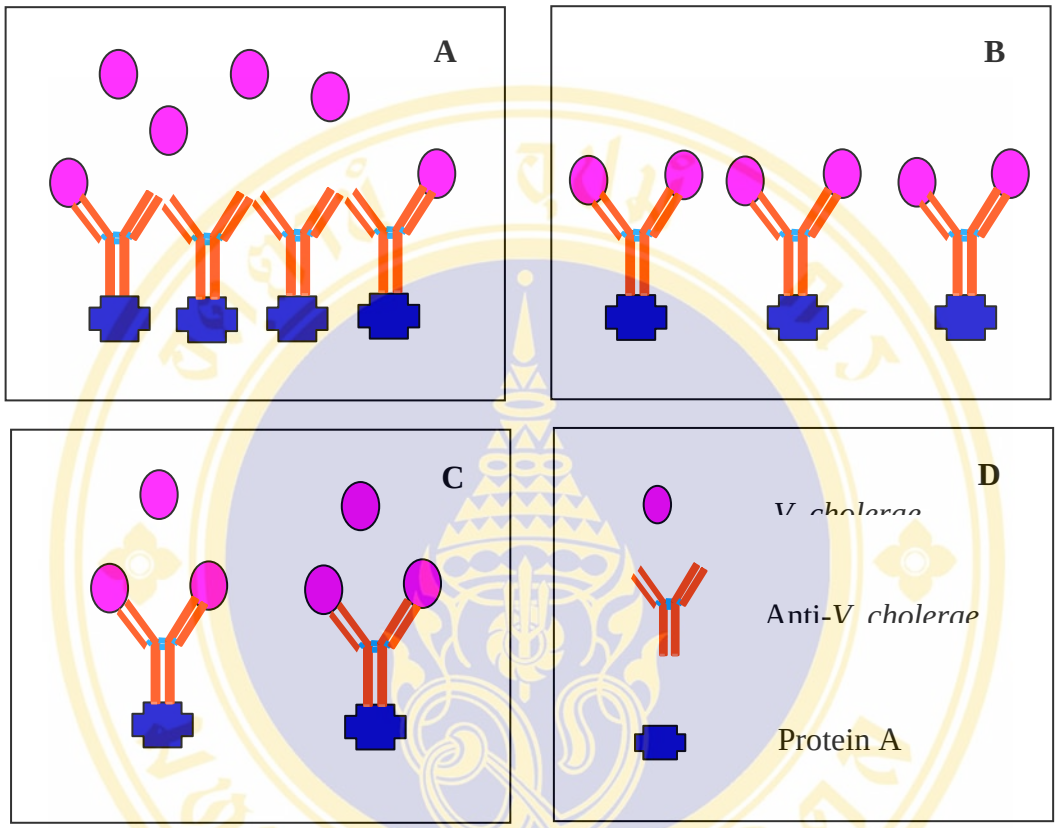


**Figure 3.7** Schematic diagram of anti-*V. cholerae* O1 on the quartz surface.

**A**: anti-*V. cholerae* O1 had little space between $F_{ab}$ so could not function antigen binding site of anti-*V. cholerae* O1 was blocked.

**B**: anti-*V. cholerae* O1 had optimal concentration.

**C**: anti-*V. cholerae* O1 were a few since *v. cholerae* O1 suspended in the specimen solution.

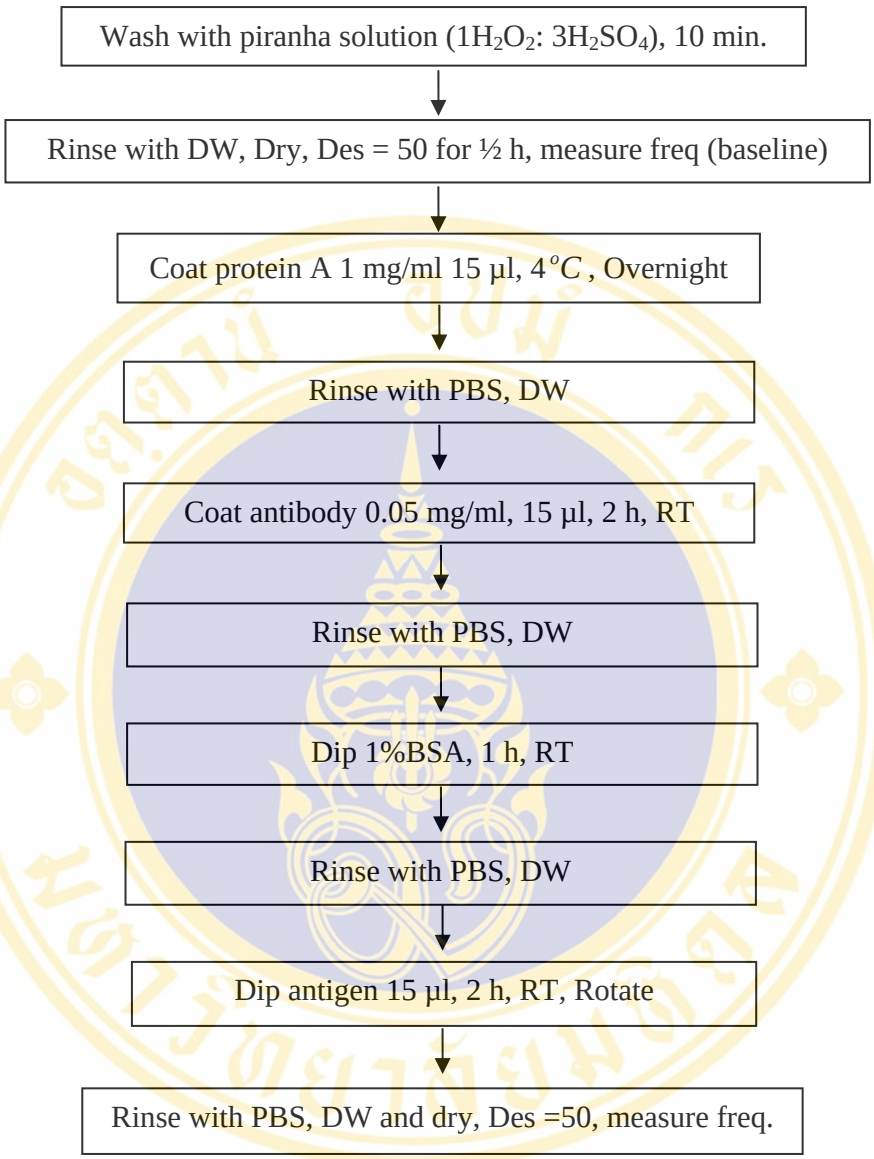


**Figure 3.8** Systematic processes of coating method for anti-*V. cholerea* O1 on the quartz surface. Crystals were cleaned with piranha solution and rinsed with distilled water and dried at room temperature (RT). Protein A was coated with 1 mg/ml 15 µl, 4 $^oC$ , overnight. Then, rinsed with PBS and distilled water before coated with varied antibody concentrations, of 15 µl for 2 h. This was then rinsed with PBS, DW and dipped into 1% BSA, for 1 h at RT. Dipped into *v. cholerea* O1 suspension, $10^8$ CFU/ml at RT for 2 h on the inverted rotator and rinsed with PBS and DW. It was put in the desiccator and measured frequency shift (Hz) was measured.

### 3.2.2.3 Detection of *V. cholerea* O1 by Piezoelectric immunosensor

The last experiment, the detection of *v. cholerae* O1 concentration from the piezoelectric immunosensor, was to study the relationship between frequency shift (Hz), $y$, and the concentration of *v. cholerae* O1 (CFU/ml), $x$. Initially, the antibody-coated sensor was dipped into 300 µl-sample of the *v. cholerae* O1 suspension on the inversed rotator rotating with slow movement. Figure 3.10 explains the procedural methodology of this experiment from the preparation of QCM to the detection of *v. cholerae* O1. The concentration of *v. cholerae* O1 suspension was diluted with normal saline at $10^4$ to $10^7$ CFU/ml to create the standard curve. Normal saline without bacteria was immobilized as the test electrode sensor but was dipped in PBS without *v. cholerae* O1. These results are displayed in Fig. 4.7.

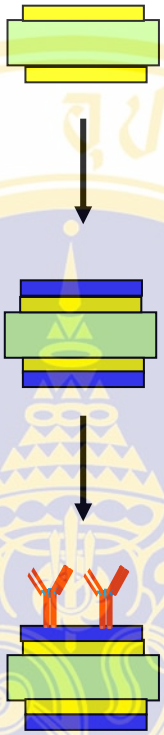

**Figure 3.9** Schematic diagram of an immunosensor device. Initially, Protein A is coated on the quartz surface. Next, anti-*V. cholerae* O1 is immobilized; $F_c$ of anti-*V. cholerae* O1 binds to protein A and $F_{ab}$ can attach specifically to *v. cholerae* O1.

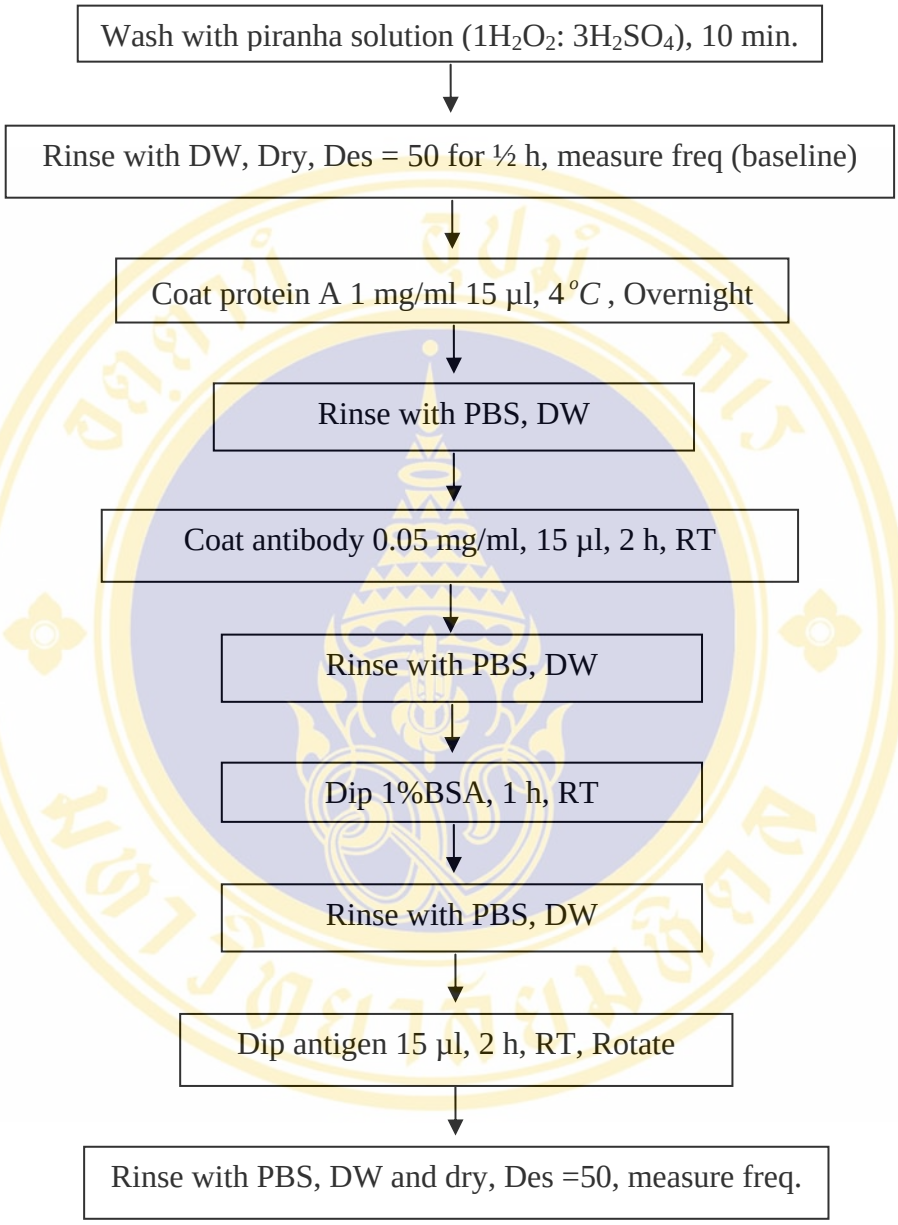


**Figure 3.10** Schematic diagram of experiment. Initially, the surface of quartz crystal was cleaned with Piranha solution for 10 min and rinsed with PBS and DW. Crystal was dried at room temperature and put in a desiccator for 0.5 h. Baseline frequency was then measured. The crystal was coated with protein A, 1 mg/ml at 4 $^oC$ overnight and rinsed just as above.

Subsequently, anti-*V. cholerae* O1 were immobilized on the quartz surface at RT for 2 h. QCM was dipped into 1%BSA solution to block the nonspecific binding from other molecules for 1 h. Then, QCM was immersed into *v. cholerae* O1 suspension on the inversed rotator and rinsed afterwards with PBS and DW. Lastly, the humidity of the QCM was controlled with desiccator for 30 min before final frequency was measured. Frequency shift which occurred from several concentrations of *v. cholerae* O1 is shown in Fig. 4.7.

# CHAPTER IV
# RESULTS

This chapter presents the results about the study of optimal detection conditions and the response curve for *v. cholerae* O1 detection by piezoimmunosensor. The study of optimal condition for *vibrio cholerae* O1 immunosensor illustrates immobilization processes. In Section 4.1, optimal conditions for coating protein A are presented. In Section 4.2, optimal conditions for immobilizing anti-*V. cholerae* O1 are presented. The last step, the response curve for *v. cholerae* O1 detection, is also shown in 4.3.

## 4.1 Determination of Optimal Conditions for Protein A Coating

This study was to determine the optimal frequency-concentration of protein A for the highest yield of protein immobilization. The degree of protein A immobilization at different concentrations is shown in Fig. 4.1. The initial immobilization yield of protein A was determined by overnight incubation at $4^{o}C$. The immobilization concentrations of protein A ranging from 0.25, 0.50, 0.75 to 1.00 mg/ml gave frequency shift of 88, 84, 85, and 125 Hz, respectively. One mg/ml (milligram per milliliter) of protein A showed the highest yield for immobilization on the crystal surface. This concentration was selected and used throughout the study.

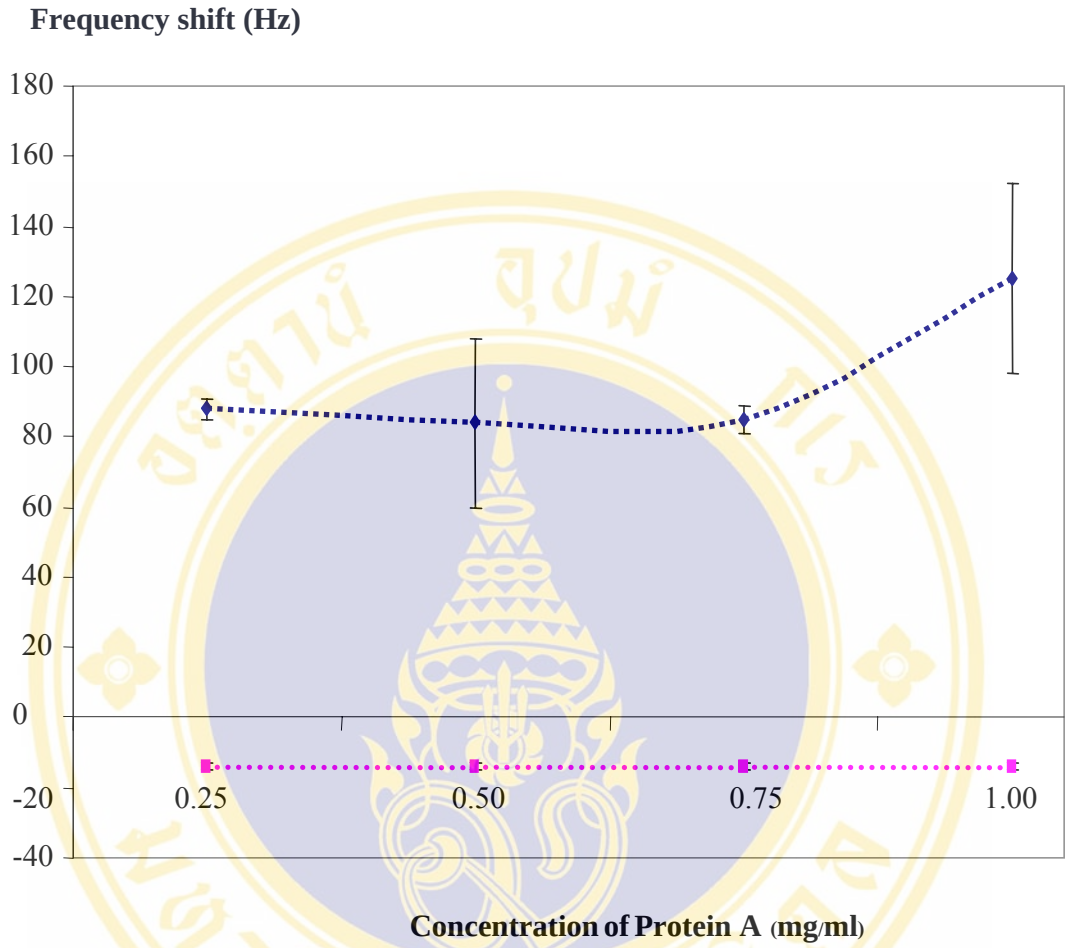


**Figure 4.1** The different concentrations of protein A ranging from 0.25, 0.05, 0.75 to 1.00 mg/ml were immobilized on the crystal surface as square dot line. The concentration of protein A, 0.25-0.75 mg/ml had frequency shift of 88, 84, and 85 Hz, respectively. One milligram per milliliter of protein A represented the highest frequency to 125 Hz and the suitable concentration in the immobilization for QCM sensor. Round dot line represented the dare crystal at 14 Hz.

## 4.2 Determination of Optimal Conditions for Immobilizing Antibodies of *Vibrio cholerae* O1

Anti-*V. cholerae* O1 used in this study were checked to see whether the antibodies bind specifically with *v. cholerae* O1 or not. Consequently, antibodies, which had affinity for the common structural antigen of *Vibrio* spp., were evaluated. The antibodies were checked for their affinities towards *v. cholerae* O1 by agglutination assay in which anti-*V. cholerae* IgG (Immunoglobulin G) agglutinated with *v. cholerae* antigen. The results in Fig. 4.2 showed an agglutination reaction by normal saline which was mixed with *v. cholerae* O1 as a negative control.

### 4.2.1 Optimal Incubation Time of Anti-*V. cholerea* O1

This experiment shown in Fig. 4.3 determined the optimal incubation time of anti-*V. cholerae* O1. Anti-*V. cholerea* O1 was incubated for 0.5, 1, 2, 4 and 8 h at room temperature giving frequency shifts of 225, 304, 392, 294 and 110 Hz, respectively. From incubation time results, anti-*V. cholerae* O1 immobilization for 2 h had the highest frequency shift. Therefore, a period of two hours was chosen for antibody immobilization throughout the study.

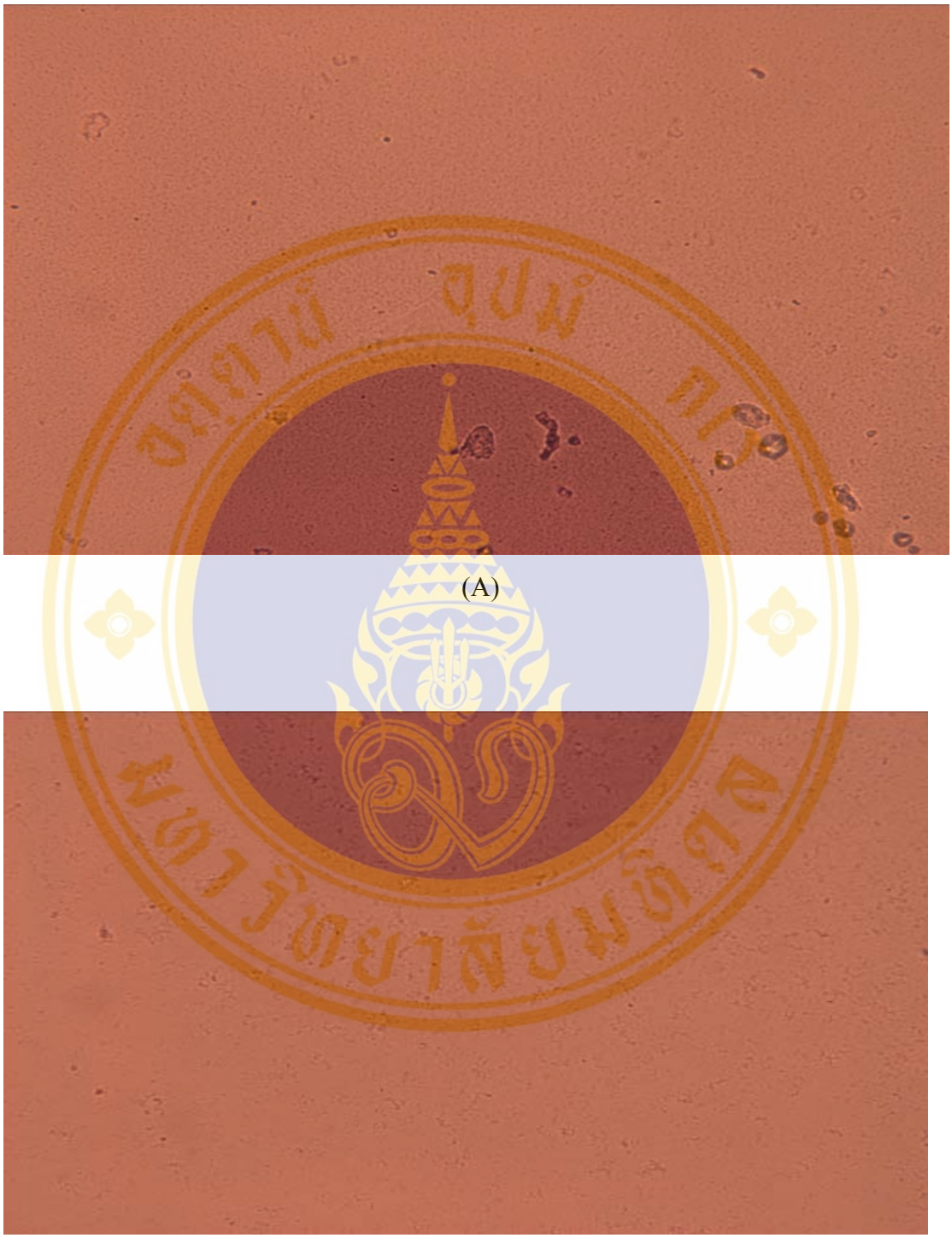

(A)

(B)

**Figure 4.2** Optical microscopic observation (x100) of agglutination reaction

**A.** Negative control: Suspension of *v. cholerae* O1 and normal saline.

**B.** Test: Agglutination of *v. cholerae* O1 and anti-*V. cholerae*.

### 4.2.2 Anti-*V. cholerae* O1 and *V. cholerae* O1 Interaction by Rotating Method

This experiment was separated into two groups: rotation and no rotation. The first group, gray colored, was activated on the inversed rotator while another group, the white, was not rotated. Each group was used to determine the frequency shift at two different anti-*V. cholerae* concentrations; 0.13 and 0.16 mg/ml. Rotated QCM showed a higher frequency shift. The rotation during antigen-antibody reaction increased antigen-antibody binding rate.

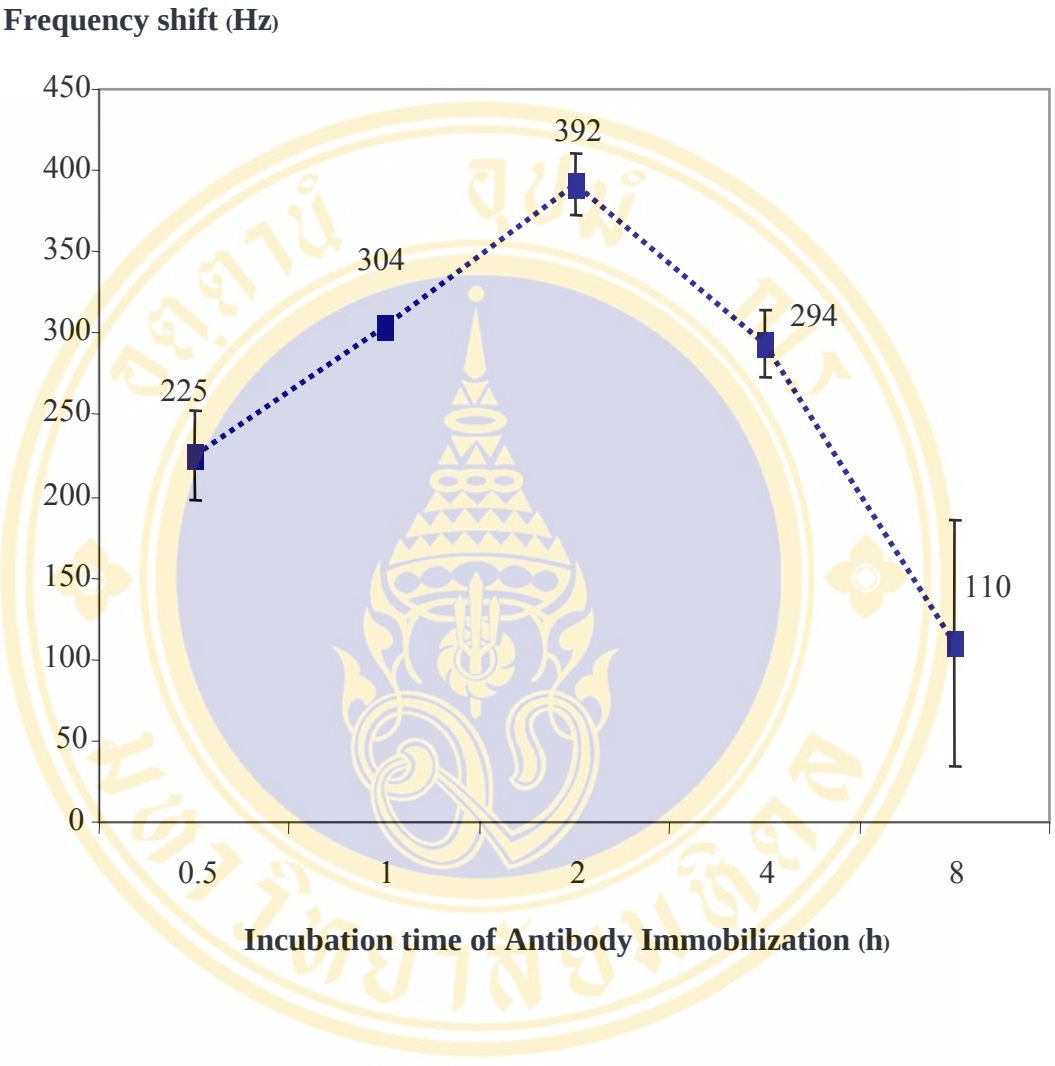


**Figure 4.3** Relationship of incubation time (h) for anti-*V. cholerea* O1 immobilization on the crystal surface and frequency shift (Hz) is showed in this curve. The X-axis presents periods of incubation time for anti-*V. cholerae* O1 immobilization. The Y-axis shows frequency shift (Hz). The optimal incubation time for anti-*V. cholerea* O1 immobilization was 2 hours which provides the highest frequency shift (392 Hz).

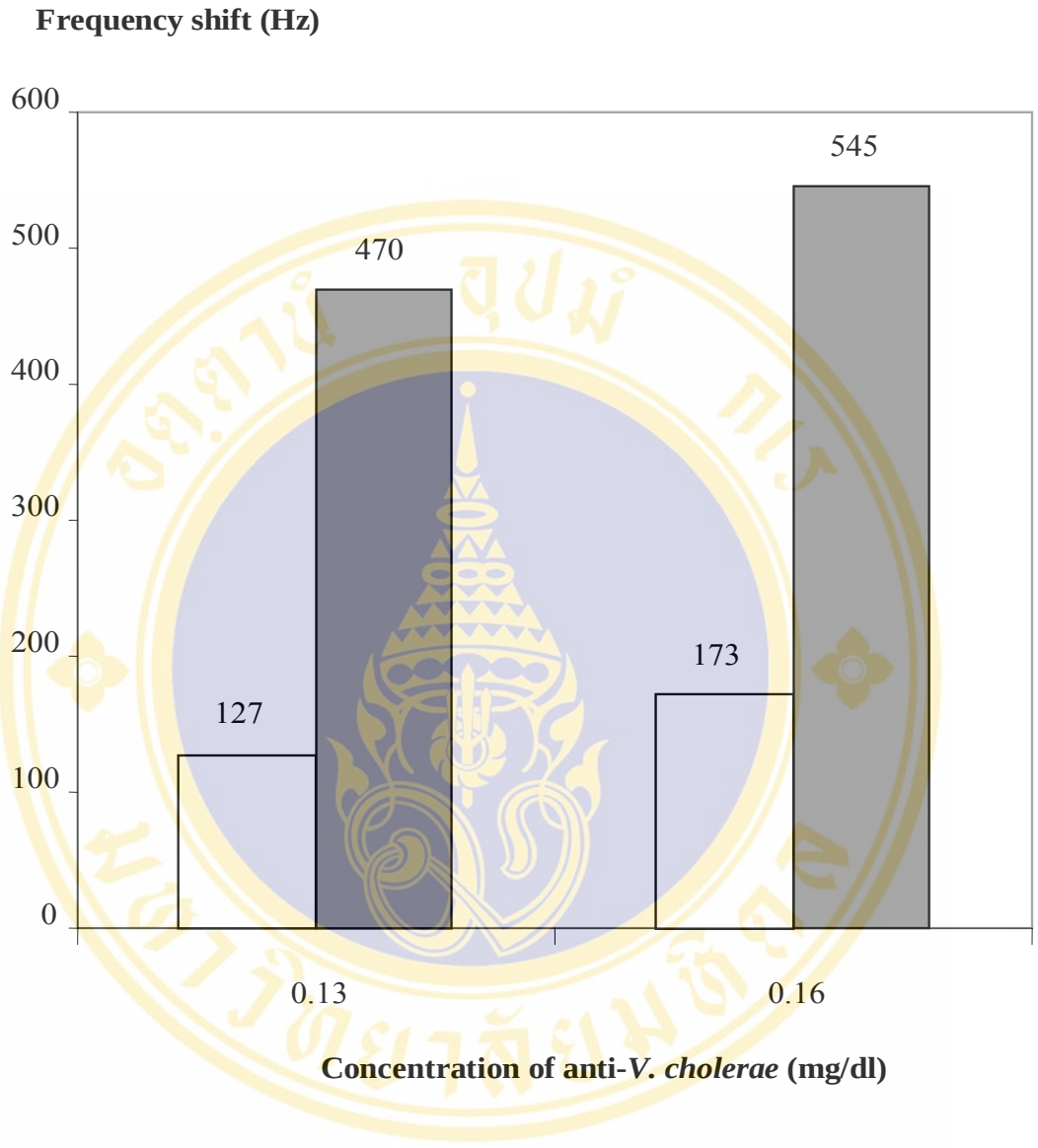


**Figure 4.4** Comparison of the rotation/ no rotation of quartz crystals immobilized with anti-*V. cholerae*, 0.13 and 0.16 mg/ml. The gray bar represents the rotated QCM and the white bar represented the no rotated QCM. A concentration, 0.13 mg/ml, of anti-*V. cholerae* presented a frequency shift to 470 Hz when rotated while the same concentration of and the no rotated QCM shifted down to 127 Hz. The frequency shift is 545 Hz and 173 Hz when rotation and no rotation (anti-*V. cholerae* O1, 0.16 mg/ml), respectively. The rotation technique helps improving the anti-*V. cholerae* O1─*V. cholerae* O1 binding.

### 4.2.3 Optimization of Anti-*V. cholerae* O1

The results for the determination of an optimal concentration of anti-*V. cholerae* O1 is presented in Fig.4.5. Antibody concentration was varied from 0.05 to 0.2 mg/ml. Frequency shift values were increased (303-451 Hz) in the range of 0.075 to 2.00 mg/ml of anti-*V. cholerae* O1, respectively. At 0.05 mg/ml, frequency shift is to 382 Hz, thus, this point could be the appropriate point because of the highest attachment of antigen-antibody complex. Frequency shift was detected using blank and negative control; Blank control is the reaction of anti-*V. cholerae* O1 and normal saline without *v. cholerae* O1. Negative control is the reaction of anti-*V. cholerae* O1 and *E. coli*. Blank control showed a frequency shift of 209 Hz. Negative control showed 297 Hz.

### 4.2.4 Optimization of Anti-*V. cholerae* O1 (continue)

The result shown in Fig.4.6 presents the optimal concentration of anti-*V. cholerae* O1 at 0.05 mg/ml. We assumed that lower concentration could increase frequency shift from antigen-antibody complex by anti-*V. cholerae* O1 dilution ranging from 0.0125 to 0.0500 mg/ml. From results listed in section 4.2.3 and section 4.2.4, we concluded that the appropriate concentration of anti-*V. cholerae* O1 was 0.05 mg/ml.

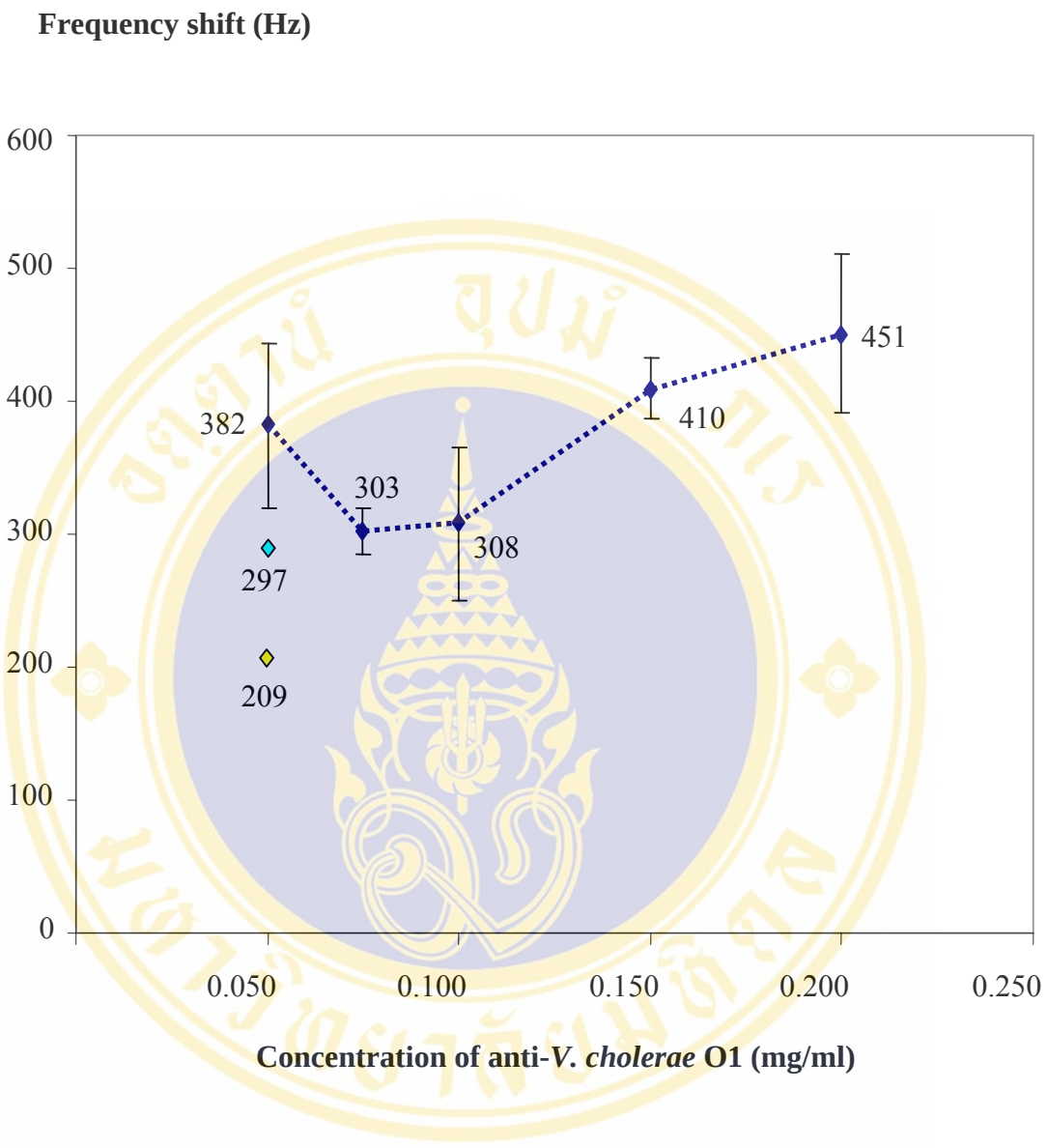


**Figure 4.5** Relationship of anti-*V. cholerae* O1 concentration (mg/ml) for immobilization on the crystal surface and frequency shift (Hz) was presented in this curve. Anti-*V. cholerae* O1 concentrations ranging from 0.05 to 0.200 mg/ml were immobilized on the quartz surface to find out the optimal anti-*V. cholerae* O1 concentration for QCM sensor. The appropriate concentration represented the highest antigen-antibody binding. Frequency shift at 382 Hz showed the suitable concentration for anti-*V. cholerae* O1 immobilization. Frequency shift at 209 Hz and 297 Hz represented blank control and negative control, respectively.

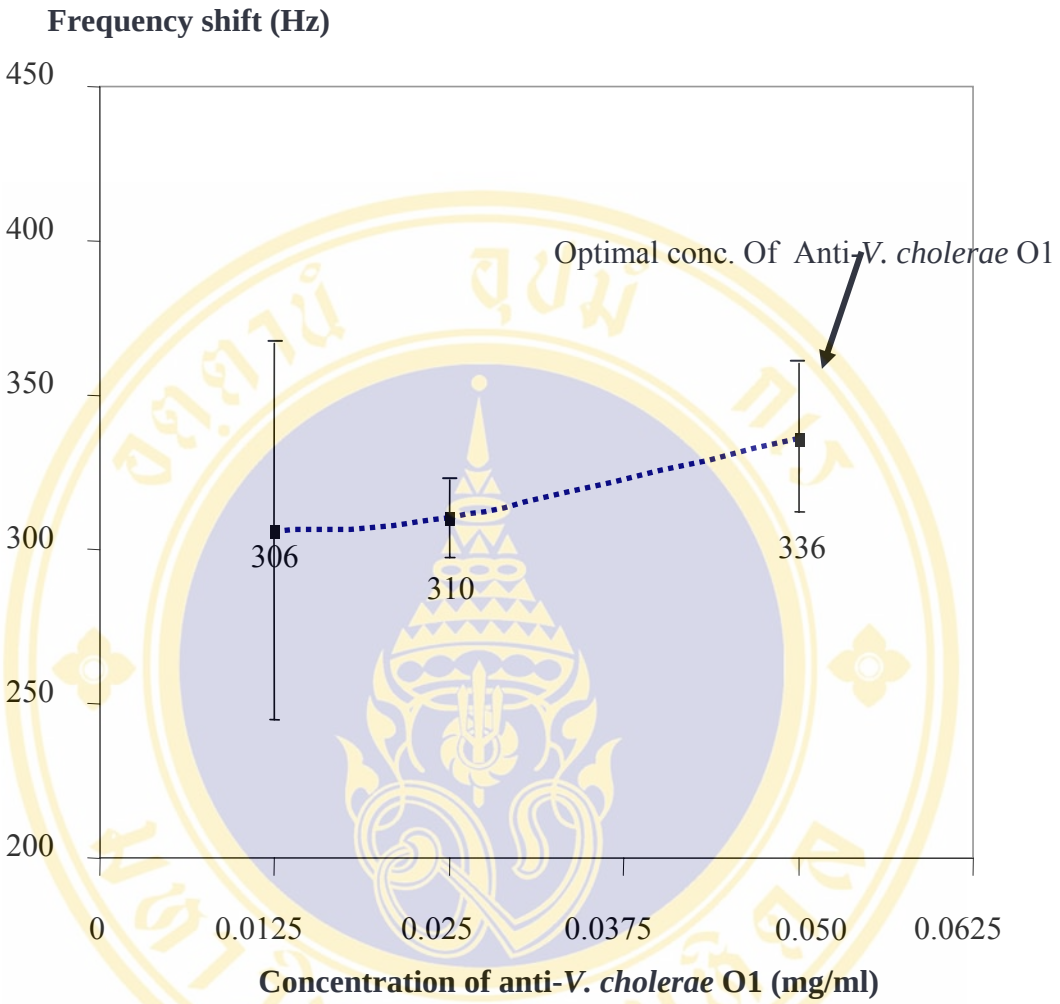


**Figure 4.6** Relationship of the immobilized anti-*V. cholerae* O1 (mg/ml) on the crystal surface and frequency shift (Hz) was showed in this curve. The anti-*V. cholerae* O1 concentrations ranging from 0.0125 to 0.0500 mg/ml were immobilized on the crystal surface to find out the appropriate anti-*V. cholerae* O1 concentration for immobilization on the quartz surface. Frequency shift at 336 Hz of anti-*V. cholerae* O1 concentration (0.05 mg/ml) presented the highest frequency that showed the highest binding between anti-*V. cholerae* O1 and *v. cholerae* O1 binding. Therefore, anti-*V. cholerae* O1 concentration (0.05 mg/ml) was the appropriate concentration for anti-*V. cholerae* O1 immobilization on the crystal surface.

### 4.3 Detection of *V. cholerea* O1 by Piezoelectric Immunosensor

Initially, *v. cholerae* O1 from agar plate was diluted by normal saline ranging from $10^1$ to $10^7$ colony forming unit per milliliter (CFU/ml). *Vibrio cholerae* O1 in normal saline was bound to anti-*V. cholerae* O1 which was immobilized on the crystal surface. These bindings caused the frequency decreasing of crystal. From these results, QCM sensor could detect *v. cholerae* O1 in range $10^4$ to $10^7$ CFU/ml, with frequency shift from 476 to 837 Hz, respectively, as showed in the Fig. 4.7. The lowest *v. cholerae* O1 concentration is $10^4$ CFU/ml, which is the most sensitive point this QCM sensor.

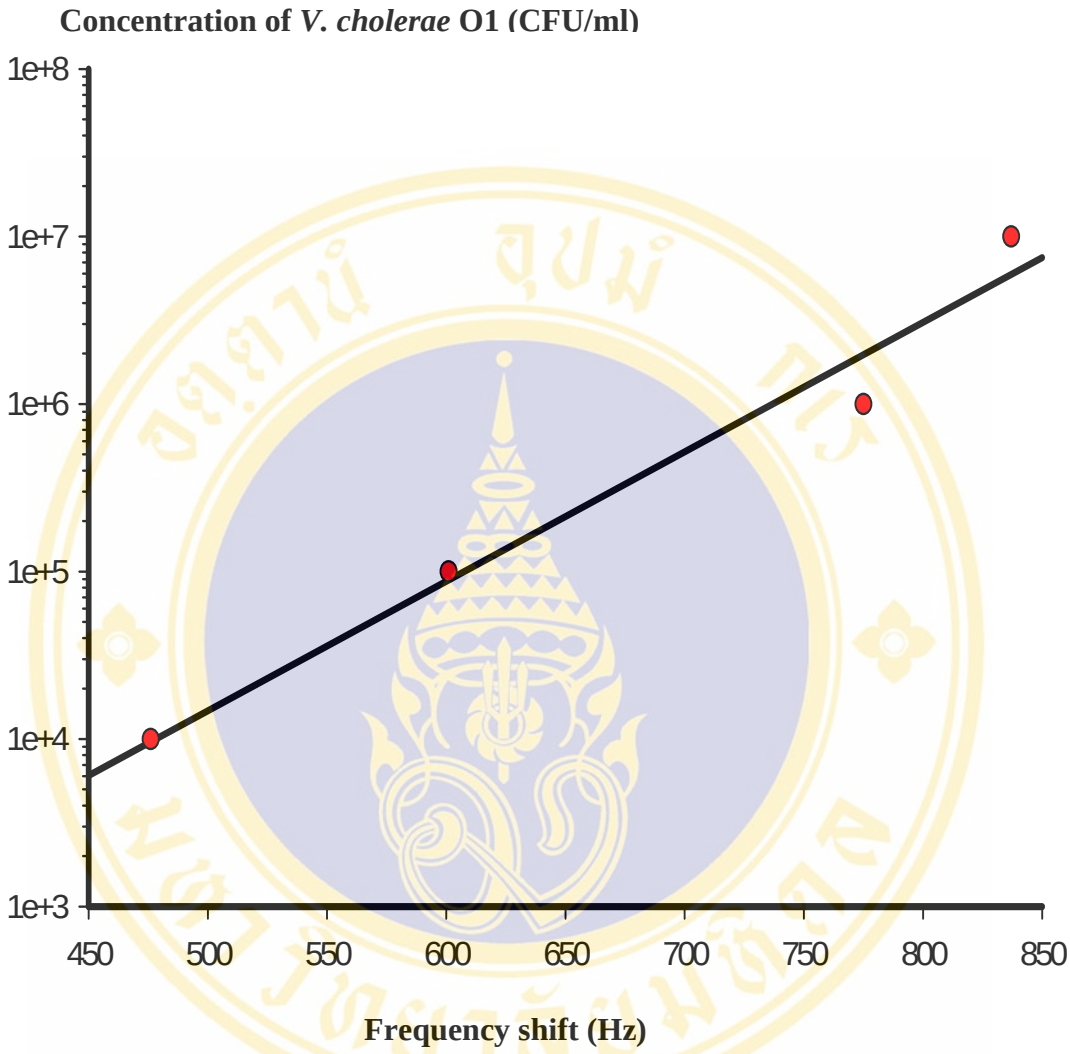


**Figure 4.7** Relationship of *v. cholerae* O1 concentration (mg/ml) and frequency shift (Hz) is showed as the straight line. The X-axis represents the *v. cholerae* O1 concentration (mg/ml). Y-axis represents the frequency shift (Hz). The QCM sensor could measure the *v. cholerae* O1 concentration in the range from $10^4$ to $10^7$ CFU/ml by frequency shift from 476 – 837 Hz. The lowest *v. cholerae* O1 concentration is $10^4$ CFU/ml.

# CHAPTER V
# DISCUSSION

This chapter discusses the results from studies in the previous chapter consisting of the electronic development in 5.1 and the biological development in 5.2. Furthermore, the PZ immunosensor was compared with the culture method as presented in 5.3.

## 5.1 Electronic Development Phase

The Piezoelectric quartz crystal with gold electrodes and the basic resonant frequency of 12 MHz are used through out these experiments. A crystal at 12 MHz is used as the electrode because it is easy to handle during immobilization. Higher frequency crystal is more fragile than lower frequency crystal because it is too thin to handle. Since AT-cut crystals have a temperature coefficient that is almost zero between 0-50 $^{o}C$, this cut type is the most suitable for QCM biosensors. The shear displacement is zero at the crystal edges, while the central quartz is maximum. The displacement at the center of the quartz, and $z = \pm d_q/2$ is maximum for the fundamental frequency where as the amplitude disappears at the quartz edges; $d_q$ is the thickness of quartz crystal. The transversal wave shows a node at $z = 0$ and maximum amplitude $z = \pm d_q/2$. The shear vibration can be described as a simple cosine function. The use of constructive interference $d_q = n\lambda/2$ and R < $d$ from Equation (9); R is the radius of quartz area which coated with gold [48].

$$f_0 = \frac{nK_R}{d_q} \qquad (9)$$

$K_R$ is called frequency constant of $AT$-cut quartz. From Equation (9), the resonance frequency of an $AT$-cut quartz increases with decreasing thickness of the crystal. For example, a 5 MHz quartz has a thickness of 0.33 mm, but a 30 MHz crystal is only 55 $\mu$m thick. Piezoelectric crystals for biosensor quartz crystal microbalance might be obtained from several companies. However, this project is the preliminary study of the QCM immunosensor thus crystals have been used to construct the piezoelectric biosensor in-house.

Oscillating circuit driving the crystal should provide enough energy to the crystal for smooth oscillation [24]. The simplest constructions are based on several papers such as the gate oscillator, 74LS320 in Fig. 2.7 of Skaldal; CMOS inverter (MC 14049) in Fig. 2.8 of Shu-Fen Chou; SN74LS124N of Andreas Janshoff, respectively. Oscillator circuit is chosen from several conditions in laboratory by focusing on high frequency stability and IC suppliers in Thailand. Therefore, the Pierce oscillator circuit is the most suitable in this study. Frequency property of Pierce oscillator can generate signal from 100 kHz to 20 MHz, especially if its frequency is above 3 MHz [94, 95]. In electronic circuit design, a crystal should be put close to the oscillation circuit to protect frequency loss.

The unit for measuring resonant frequency changes uses common components widely used in electronics. The indirect counting method is used for counting much higher stable frequency. This approach provides a short measuring time and a better resolution. A PIC-microcontroller consists of many timers counting clock signals to convert the resonant frequency and interfaces to an LCD or personal computer in order to allow on-line monitoring of the interaction on the quartz surface.

Over the last decade extensive research efforts in the area of piezoelectric biosensors have resulted in the development of broad theoretical and experimental knowledge. However, these successful QCM-researches have not yet led to wide commercial success. The transfer of QCM biosensor concepts from the laboratory to the market has been very limited. Piezoelectric biosensors require specific design concepts which are related to the nature of a piezoelectric transducer- biological film- enclosure interface as shown in Fig. 5.1 [32]. This model presents a complete biosensor scheme in addition to a sensing process, signal processing and packing units. *V. cholerae* O1 is exposed to the anti-*V. cholerae* O1 which is selective to the antigen of interest.

Frequency shift of QCM occurs as mass changes on the quartz surface are converted by the physical transducer into an output electric signal. The electric signal is conditioned, processed and displayed. Therefore, the sensing section and sensing process can be included in a portable packaging unit. Design of these elements is essential for the development of marketable biosensors. Furthermore, the commercial instruments manufactured at present are not portable.

## 5.2 Biological Development Phase

This part compiles of the first discussion about the optimal conditions for protein A coating in Section 5.2.1, and the second discussion about the optimal conditions for anti-*V. cholerae* O1 in Section 5.2.2. The optimal incubation time, the increasing attachment technique, and the optimal anti-*V. cholerae* O1 concentration are discussed in Sections 5.2.2.1, 5.2.2.2, and 5.2.2.3, respectively. Discussion about *V. cholerae* O1 detection by piezoelectric immunosensor is explained in Section 5.2.3. The last discussion is about comparison between PZ immunosensor and the other methods in Section 5.2.4

### 5.2.1 The Optimal Conditions for Protein A Coating

Protein A is the most popular chemical reagent for antibody immobilization. It is a cell wall protein, produced by strains of *Staphylococcus aureus*, which exists as a single polypeptide chain of molecular weighted 42,000 Da and has a much extended shape [96]. From Literature Review in Chapter II, Fig. 2.10 shows the attachment of an antibody to a chemical compound. Protein A as chemical compound is a directed immobilization method due to its natural affinity towards the $F_c$ region of IgG (Immunoglobulin G: antibody) molecules. Thus, $F_{ab}$ of antibody can attach itself to a suitable antigen. Gold- Protein A complex is highly stable with Van der Waals bond. The study is to determine the optimal protein A concentration from the highest yield of protein A. Table 1 in the Appendix indicates that the optimal concentration of protein A is 1 mg/ml which gives the highest frequency, and then the highest yield as shown in Table 2. Xiao-Li Su and Yanbin Li used 1mg/ml of protein A for *Salmonella* detection

[89]. Xia Chu *et al* recommended the solution of protein A, 1 mg/ml was applied on the surface of the gold crystal [90]. Changes in the resonant frequency of the quartz crystal can be converted to changes in mass by using Sauerbrey's equation. Table 2 showed the calculated mass changes derived from changes in resonant frequency of the quartz crystal oscillator obtained using protein A immobilization. The change in mass corresponds to the protein A molecules deposited on the electrode. Protein A, 1 mg/ml corresponds the highest frequency that the protein A volume is the highest immobilized on the crystal surface. It is possible that protein A (1 mg/ml) binds the anti-*V. cholerae* O1 better than other protein A concentrations like as Xia Chu and Yabin Li.

### 5.2.2 The Optimal Conditions for Immobilization Anti-*V. cholerae* O1

Many immobilization methods have been proposed using piezoelectric biosensors, but there is no method that gives high immobilization and good stability. For this reason, it is necessary to find out a suitable immobilization method for anti-*V. cholerae* O1. The study of anti-*V. cholerae* O1 in immobilization techniques is considered from (1) the best anti-*V. cholerae* O1 for immobilization; (2) the optimal immobilization parameters (Incubation time, concentration or etc) for the highest yield of the attached QCM layer; (3) the noise effect of the immobilization layers on the frequency and surface characteristics of the quartz crystal. The results of these individual studies could help to select the best immobilization process.

This part discuss about the affinity of anti-*V. cholerae* O1 to *v. cholerae* O1 by agglutination technique in Section 5.2.2.1, then the optimal incubation time of anti-*V. cholerae* O1 for immobilization in Section 5.2.2.2. The rotation method increasing the anti-*V. cholerae* O1 and *v. cholerae* O1 attachment was discussed in Section 5.2.2.3. Moreover, the optimization of anti-*V. cholerae* O1 was presented in Section 5.2.2.4.

#### 5.2.2.1 Anti-*V. cholerae* O1 and *V. cholerae* O1 reaction

Protein A was immobilized in the first layer on the quartz surface, then anti-*V. cholerae* O1 was immobilized in the second layer as shown in Fig. 5.1. Anti-*V. cholerae* O1 are tested for affinity towards *v. cholerae* O1 by agglutination

process. Figure 4.2B shows agglutination between *v. cholerae* O1 and anti-*V. cholerae* O1. Anti-*V. cholerae* O1 binds *v. cholerae* O1 with high specificity. We found that there was sediments of anti-*V. cholerae* O1—*v. cholerae* O1 binding over the glass slide. Sediments were the agglutination between the antigen binding sites of anti-*V. cholerae* O1 and the epitope of *v. cholerae* O1 as shown in Fig. 5.2. On the contrary, Figure 4.2 A showed *V. cholerae* O1 cell floated in normal saline solution. There was not binding of anti-*V. cholerae* O1 and *v. cholerae* O1.

#### 5.2.2.2 The Optimal Incubation Time of Anti-*V. cholerae* O1

The incubation time of anti-*V. cholerae* O1 immobilization affected frequency signal. The optimal incubation time of anti-*V. cholerae* O1 immobilization of 2 h offers the highest frequency shift showed in Fig. 4.3. For 0.5 and 1 h of anti-*V. cholerae* O1 incubation time gave a low frequency shift. It is possible that anti-*V. cholerae* O1 immobilization is not completed on the crystal surface. The antibody concentration (0.5 mg/ml) is immobilized completely by using anti-*V. cholerae* O1 incubation time for 2 h at room temperature (22-25$^{o}C$ ). After 2 h, antibodies reduce the affinity of the binding with antigens It is possible that anti-*V. cholerae* O1 is kept in the room temperature for a long time over 2 h. Antibody may denature. This result is seemed to the Babacans' work. Babacan presented the 2 h at 22$^{o}C$ gave the highest antibody immobilization [96]. Moreover, Babacan presented that a low temperature-long incubation time combination worked better for non-covalent interaction. It is probable that this combination provided less energetic and more stable conditions for the molecules to interact. Low temperature-long incubation time combinations are also found to work better for the non-covalent binding steps of ELISA protocols used in the selection of the most effective antibody.

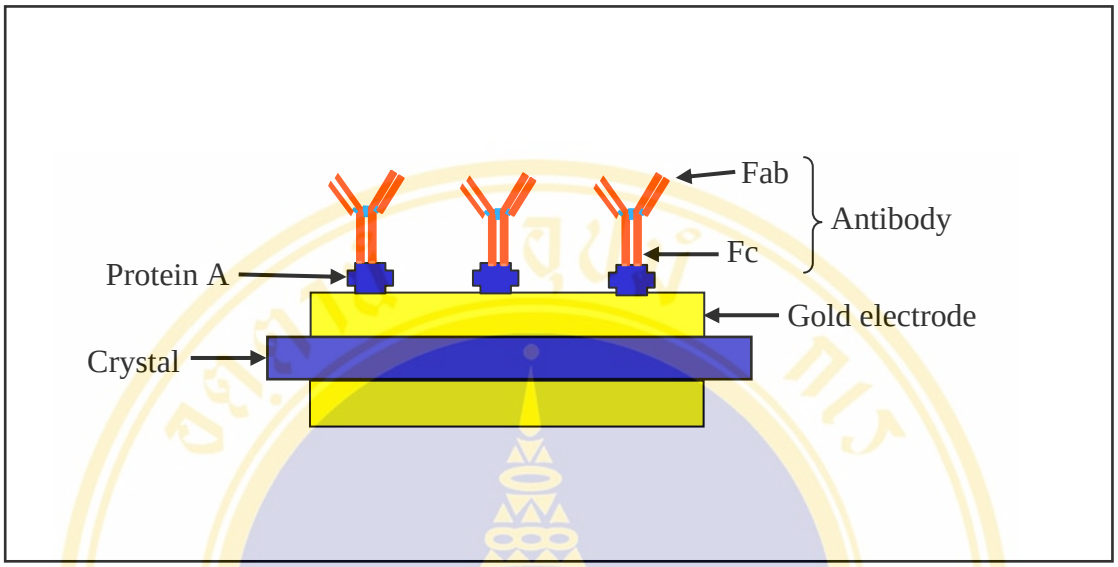


**Figure 5.1** Protein A coating

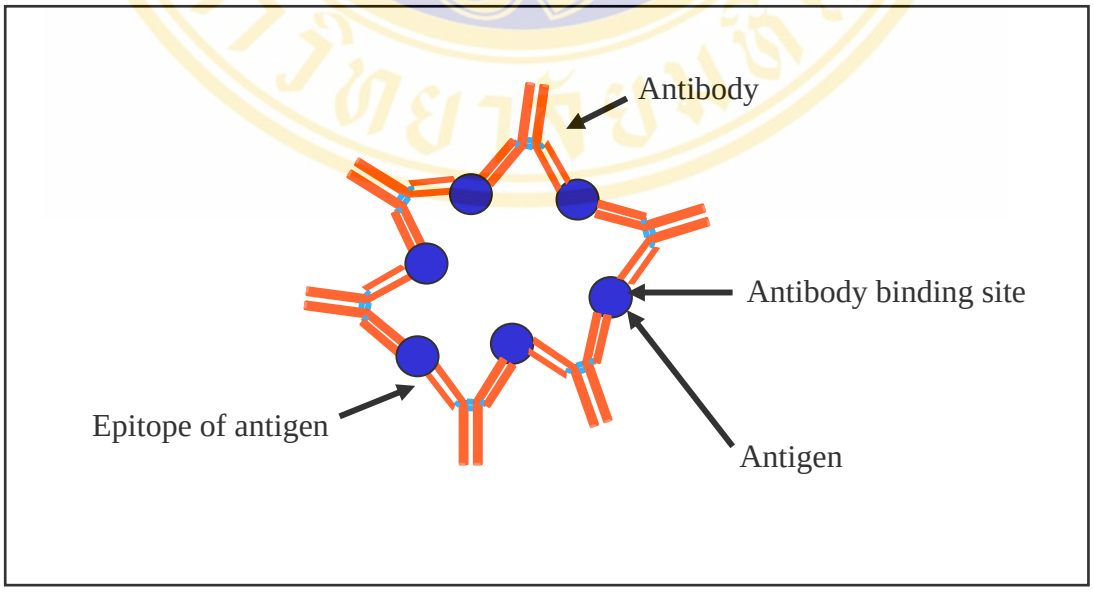


**Figure 5.2** Antigen-antibody binding

#### 5.2.2.3 Anti-*V. cholerae* O1 and *V. cholerae* O1 Interaction by Rotating Method

The rotated QCM during anti-*V. cholerae* O1 — *v. cholerae* O1 reaction is higher than the no rotated QCM. *Vibrio cholerae* O1 size has bigger than anti-*V. cholerae* O1 size, so the binding between anti-*V. cholerae* O1 and *v. cholerae* O1 is difficult. It is possible that the rotation increases *v. cholerae* O1 movement since *v. cholerae* O1 binds to anti- *V. cholerae* O1 easily on the crystal surface. On the contrary, frequency shift of the no rotated QCM was near the frequency shift of protein A coating. It is possible that the no rotated QCM does not occur the binding between anti-*V. cholerae* O1 and *v. cholerae* O1 on the crystal surface. Rotation method does not only improve chance for these combinations, but also amplify frequency signal significantly. The rotation method is the important method for using QCM sensor in *v. cholerae* O1 detection.

#### 5.2.2.4 The Optimization of Anti-*V. cholerae* O1

Attachment and spreading of antibodies on the quartz surface are complex processes. From Fig. 4.5 that showed the highest frequency shift of antibody concentration at 0.05 mg/ml. In experiment, various concentrations of anti-*V. cholerae* O1 are applied from 0.075 to 0.200 mg/ml on the quartz surface. Mass loading of anti-*V. cholerae* O1 on crystal surface shifts to the concentration of anti-*V. cholerae* O1. Anti-*V. cholerae* O1, 0.05 mg/ml, showed the higher frequency shift than other anti- *V. cholerae* O1 concentrations. It is possible that anti-*V. cholerae* O1 concentration (0.05 mg/ml) is immobilized by suitable space of the antigen binding site($F_{ab}$). Therefore, $F_{ab}$ of anti-*V. cholerae* O1 can bind to epitope of *v. cholerae* O1. On the contrary, anti-*V. cholerae* O1 concentrations (0.15 and 0.20 mg/ml) were higher frequency shift than 0.05 mg/ml. It is possible that anti-*V. cholerae* O1 (0.15-0.20 mg/ml) are over immobilized on the crystal surface until $F_{ab}$ of anti-*V. cholerae* O1 cannot bind to epitope of *v. cholerae* O1.

Blank control: anti-*V. cholerae* O1 did not immobilized on the quartz surface, thus the agglutination between *v. cholerae* O1 and anti-*V. cholerae* O1 complex did not occur. Blank control gave the lowest frequency because its frequency came from mass of protein A coating. Negative control (*E. coli*) found that the frequency of negative control was higher than frequency of blank because there was mass of protein A and anti-*V. cholerae* O1 on the crystal surface. Negative control showed that QCM immunosensor did not cross reaction with other bacteria (*E. coli*). Thus, the QCM sensor presented to specific to *v. cholerae* O1.

. Figure 4.6 presents the optimal concentration of anti-*V. cholerae* O1 ranging from 0.0125 to 0.05 mg/ml. Concentrations of anti-*V. cholerae* O1, 0.0125 and 0.025 mg/ml showed fewer frequency than 0.05 mg/ml of anti-*V. cholerae* O1 concentrations. It is possible that the number of anti-*V. cholerae* O1 (0.0125,0.025 mg/ml) is lower than the number of anti-*V. cholerae* O1 (0.05 mg/ml). The anti-*V. cholerae* O1— *v. cholerae* O1 binding of anti-*V. cholerae* O1 concentration (0.0125,0.025 mg/ml) will be lower than the anti-*V. cholerae* O1— *v. cholerae* O1 binding of anti-*V. cholerae* O1 concentration (0.05 mg/ml). From results of Fig. 4.5 and 4.6 demonstrate that the concentration of anti-*V. cholerae* O1, 0.05 mg/ml, is the suitable anti-*V. cholerae* O1 for immobilization on the crystal surface; hence we used this anti-*V. cholerae* O1 concentration for *v. cholerae* O1 antigen detection in the next experiment.

### 5.2.3 Detection of *V. cholerae* O1 by Piezoelectric Immunosensor

A calibration curve for *v. cholerae* O1 concentration in suspension is shown in Fig. 4.7. A linear relationship existed between the frequency shift (Hz); X-axis and concentrations of *v. cholerae* O1 concentration (CFU/ml); Y-axis. The QCM immunosensor can detect *v. cholerae* O1 concentration from $10^4$ to $10^7$ CFU/ml. The QCM sensor cannot detect the *v. cholerae* O1 concentrations which are lower than $10^4$ CFU/ml of *v. cholerae* O1. It is possible that *v. cholerae* O1 volume is a few until QCM does not detect it. If the *v. cholerae* O1 concentrations are higher than $10^7$ CFU/ml of *v. cholerae* O1 concentration, anti-*V. cholerae O1* are closely immobilized until $F_{ab}$ of

anti-*V. cholerae O1* cannot bind *v. cholerae* O1. QCM sensor presented the most sensitivity at $10^4$ CFU/ml.

### 5.2.4 Comparing between Piezoelectric Immunosensor and Other Methods for *V. cholerae* O1 Detection

The piezoelectric immunosensor has many advantages such as time detection, low cost, and portability. The culture method uses time for bacteria detection about 2-3 days whereas PZ immunosensor can detect bacteria in less than 1 day. Therefore, the doctor can treat antibiotic drug for patients rapidly for rescuing many the patients' life. Piezoelectric immunosensor is developed from the general electronic part so price of PZ instrument is too cheap especially for producing mass product. However, the culture method uses many agars for bacteria growth and uses special agars in bacteria identification. The special agars are much expensive; hence the microscopic laboratories are limited of bacteria analysis by followed up budget of hospital. The design for portable biosensors is the important point of this study because the doctor can bring PZ immunosensor to treat the remote patients. The culture method is consisted of many instruments such as an incubator, a Hazard Hood, and etc.

ELISA is one method of *v. cholerae* O1 detections. This method is high sensitivity and specificity. However, this method has disadvantages from expensive reagents and equipment in working process. PZ immunosensor does not require labeling, which is the obvious advantage when compared with ELISA. Other advantage of PZ immunosensor is that it is reusable with no noticeable degradation in performance [97]. In addition, piezoelectric immunosensor can operate in optically opaque media. Furthermore, PZ immunosensor is inexpensive, easy-to-use and feature rapid response, hence it may allow for wide screenings and the development of effective preventive strategies for a board range of disease in the recent time.

# CHAPTER VI
# CONCLUSION

The QCM immunosensor was designed for rapid detection of *vibrio cholerae* O1 using anti-*V. cholerae* O1. The optimal concentration of protein A for antibody immobilization on the crystal surface was 1.0 mg/ml at 22-25 $^{o}C$. The optimal concentration of anti-*V. cholerae* O1 was 0.05 mg/ml by immobilization for 2 h. Furthermore, this QCM immunosensor offers high sensitivity up to $10^4$ CFU/ml for *v. cholerae* O1 detection. This research found that the rotation during anti-*V. cholerae* O1—*v. cholerae* O1 reaction helps to improve anti-*V. cholerae* O1—*v. cholerae* O1 binding.

The QCM immunosensor achieves the objectives higher sensitivity, higher specificity, and lower cost when compared with culture method. The QCM immunosensor is the fundamental biosensor for bacteria detection in Thailand. Moreover, an error study will be used as a foundation for further development of other immunosensors based on piezoelectric for pathogen diagnosis. This immunosensor is designed to detect bacteria in gas phase, thus it is not suitable for using with specimens which are in liquid phase. Therefore, QCM immunosensor would be improved by adding the flow cell for sample injection. The QCM immunosensor is the smart immunosensor for the future.

# REFERENCES


1. Finkelstein RA. *Vibrio cholerae* O1 and O139, and Other Pathogenic Vibrios, http://www.cfsph.iastate.edu/Factsheets/pdfs/cholera.pdf.
2. S.F. D'Souza. Review Microbrial biosensors. J Biosens Bioelectron 2001; 16: 337-53.
3. World Health Organization. Global Task Force on Cholera Control, Guidelines for cholera control. Geneva: WHO; 1992. Publication no. WHO/ CDD/ SER/ 80.4Rev.4.
4. World Health Organization. Epedemic diarrhoeal disease preparedness and response: training and practice. Participant's manual. Geneva: WHO; 1997. Publication no. WHO/ EMC/ DIS/ 97.3.
5. Dorothy JF. Clinical Immunology Principle and Laboratory Diagnosis, 2nd. Sheenhan C. (eds). Lippincott, Philadephia, NY; 89-100.
6. Deshpande SS, Antibodies:Biochemistry, structure, and function. In:Enzyme Immunoassays: From Concept to Product Development. Chapman and Hill, NY, 24-51.
7. Nicola CF, Jane EF, Monika JG.. Immobilized Biomolecules in Analysis: A practical approach. Cass T, Ligles FS (eds) Oxford University Press Inc., NY; 97-100.
8. Turner M, Immunology. 6th 2001. Roitt I, Brostoff J, Male D (eds). Mosby, A harcout Health Sciences Company, London: 65-80.
9. Baxter GA, Oconnor MC, Haughey SA, Crooks SRH, Elliott CT. Evaluation of an immunobiosensor for the on-site testing of veterinary drug residues at an abattoir. Screening for sulfamethazine in pigs. J Analyst 1999; 124(9): 1315-18.
10. Carlson MA, Bargeron CB, Benson DC, et al. An automated, handheld biosensor for aflatoxin. J Biosens Bioelectron 2000; 14: 841-8.

11. Dill K, Stanker LH, Young CR. Detection of salmonella in poultry using a silicon chip-based biosensor. J Biochem Biophys 1999; 41: 61-7.
12. Elliot CT, Baxter GA, Hewitt SA, *et al.* Use of biosensors for rapid drug residue analysis without sample deconjugation or clean up: a possible way forward. J Analyst 1998; 123(12): 2469-73.
13. Esti M, Volpe G, Massignan L, *et al.* Determination of amines in fresh and modified atmosphere packaged fruits using electrochemical biosensors. J Agricultural and Food Chem 1998; 46(10): 4233-37.
14. Kumar A. Biosensors based on piezoelectric crystal detectors. http:// www.tms.org/pubs/journals/JOM/0010/Kumar/Kumar-0010.htmc
15. Su XD, Li SFY, Kwang J, Low S. Piezoelectric quartz crystal based screening test for porcine reproductive and respiratory syndrome virus infection in pigs. J Analyst 2000; 125(4): 725-30.
16. Abullah J, Ahmad M, Karuppiah N, Heng LY, Sidek H. Immobilization of tyrosinase in chitosan film for an optical detection of phenol. J Sensors and Actuators B 2006; 114(2): 604-9.
17. Velasco-Garcia MN and Mottran T. Review paper Biosensor Technology addressing Agricultural Problems. J Biosystems Engineering 2003; 84 (1): 1-12.
18. Kurosawa S, Han DS, Aizawa H, Yoshimoto M, et al. Gas sensor using high-frequency quartz crystal microbalance Proc. 2001 IEEE Int. Frequency Control Symp. And PDA Exhibition (Seattle: IEEE), 462-4.
19. Kurosawa S. Development of a novel determination method for dioxin concentration enables more accurate and rapid dioxin determination than using the JIS method Press release of AIST. http://www.aist.go.jp/asit_e/new_reserch/2002/20020717/20020717.html.
20. Carr PW, Bowers LD. In Immobilized Enzymes in Analytical and Clinical Chemistry. Elving PJ, Winefordner JD (eds). John Wiley Inc., NY;68 :254.
21. Kumagai I, Tsumoto K. Antigen-antibody binding. Encyclopedia of life science. Nature Publishing Group; 2001.
22. Ebato H, Gentry CA, Herron JN, *et al.* Investigation of specific binding of antifluorescyl antibody and Fab to fluorescein lipids in Langmuir-Blodgett

deposited films using quartz crystal microbalance methodology. J Anal Chem 1994; 66: 1683-9.

23. Atassi MZ, Van Oss CJ, Absolom DR. Translated by C. Zheng, A. Wu. Molecular immunology. Beijing: Science Press; 1988.
24. Skáldal P. Piezoelectric Quartz Crystal Sensors Applied for Bioanalytical Assays and Characterization of Affinity Interactions. J Braz Chem Soc 2003; 14: 491-502.
25. Yao S, Zhou T. Dependence of the oscillation frequency of a piezoelectric crystal on the physical properties of liquid. J Anal Chim Acta 1988; 212: 61- 72.
26. Kanazawa KK, Gordon II JG. The oscillation frequency of a quartz resonator in contact with a liquid. J Anal Chim Acta 1985; 175: 99-105.
27. Xie Q, Wang J, Zhou A, Zhang Y, Liu H, Xu Z, et al. A study of depletion layer effects on equivalent circuit parameters using and electrochemical quartz crystal impedance system. J Anal Chem Acta 1999; 71: 4649-56.
28. Su XL, Li Y. A self-assembled monolayer-based piezoelectric immunosensor for rapid detection of *Escherichia coli* O157:H7. J Biosens Bioelectron 2004; 19: 563-74.
29. Park IS, Kim N. Thiolated Salmonella antibody immobilization onto the gold surface of piezoelectric quartz crystal. J Biosens Bioelectron 1998; 13: 1091-7.
30. Chou SF, Hsu WL, Hwang JM, Chen CY. Determine of α-Fetoprotein in Human Serum by a Quartz Crystal Microbalance-based Immunosensor. J Clin Chem 2002; 48: 913-8.
31. Kumar A, *et al.* Design and Implementation of a Piezoelectric Biosensors for Multifunctional Applications, Integrated Design and Process Technology. IDPT 1998; 1: 35-41.
32. Lec R M. Piezoelectric biosensors: recent advances and applications. IEEE sensors 2001; 419-29.
33. Ballantaine DS, White RM, Martin SJ, Ricco AJ, Zellers ET, Frye GC and Wohltjen. Acoustic Wave Sensors. Academic Press, 1997.

34. Lec RM, LEwin PA. Acoustic Wave Biosensors, Porceeding of 20th Annuanl IEEE Engineering in Medicine and Biology Society 1998; 20(6), 2785-90.
35. Vellekoop M. Acoustic Wave Sensors And Their Technology. J Ultrasonics 1998; 36: 7-14.
36. McHale G, Newton MI, Banerjee MK, Cowen JA. Acoustic Wave-Liquid Interactions. J Materials Science Engineering C 2000; 12: 17-22.
37. Josse F, Dahint R, Schmacher J, Grunze, Andale JC, Vetelino JF. On the Mass Sensitivity of Acoustic-Plate-Mode sensors. J Sensors and Actuators A 1996; 53: 243-8.
38. Vig J, Quartz Crystal Resonators and Oscillators. A tutorial http://www. IEEE-uffc.org/freqcontrol/tutorials/
39. Ballato A. Piezoelectricity: Old Effect, New Thrust, IEEE Trans.Ultrason., Ferroelec., Freq.Contr. 1995; 42: 916-26.
40. Lucklum R, Behling C, Hauptmann P. Role of Mass Accumulation and Viscoelastic Film Properties for the Response of Acoustic-Wave-Based Chemical Sensors. 1999; 71: 2488-96.
41. Behling C, Lucklum R, Haupptmann P. Response of quartz-crystal resonators to gas and liquid analyte exposure. J Sensor and Actuators A 1998; 68: 388-98.
42. Urbakh M, Daikhin L. Surface Morphology and The Quartz Crystal microbalance response in Liquids. J Colliods and Surfaces A 1998; 134: 75-84.
43. Schneider TW, Martin SJ, Influence of Compressional Wave Generation on Thickness-Shear Mode resonator Responses in a Fluid. J Anal Chim Acta 1995; 65(18), 3324-35.
44. Eichelbaum F, Borngraber R, Schhroder J, Lucklum R. Interface Circuits for Quartz-Crystal Microbalance Sensors. Review of Scientific Instruments 1999; 70(5): 2-11.
45. Schweyer M, Weaver J, Andle JC, McAllister D, French L, Vetelino J. Comparison of Surface Transverse Wave (STW) and Shear Horizontal Acoustic Plate Mode (SHAPM) Device for Biochemical Sensors. Proc. Of the

1997 IEEE International Frequency Control Symposium, Kansas City, MO, 2000: 147-55.

46. Benes E, Groshl M, Burger W, Schmid M. Sensors Based on piezoelectric resonators. J Sensors and Actuator 1995; 45: 1-21.
47. Rickert j, Weiss T, Kraas W, Jung G, Gopel W. A new affinity biosensor: self-assembled thiols as selective monolayers coating of quartz crystal microbalances. J Biosens Bioelectron 1996; 11: 591-8.
48. Janshoff A, Galla H-J, Steinem C. Piezoelectric Mass-Sensing Devices as Biosensors-An Alternative to Optical Biosensors. Angrew Chem Int Ed 2000; 39: 4004-4032.
49. O' Sullian CK and Guibault GG. Review: Commercial quartz crystal microbalance-theory and applications. J Biosens Bioelectron 1999; 14: 663-670.
50. Ebersole R. PZ quartz sensors for use in clinical analysis. J Am Chem Soc 1990; 112: 3239.
51. Ehahoun H, Gabrielli C, Keddam M, Perrot H, Cetre Y, Diguet L. Electrochemical quartz crystal microbalance corrosion sensor for solid metals and metal alloys: application to the dissolution of 304 stainless steel. J Electrochem Soc 2001; 148.
52. Andle JF, Schwyer M, French L, Vetelino J. Experimental Acoustic Plate Mode Properties of Y-cut Quartz. Proc. Of the 1996 UFFC Symposium 1996; 532-40.
53. Martin SJ, Bandey HL, Cernosek RW. Equivalent circuit model for the thickness shear mode resonators. J Anal Chem Acta 2000; 72: 141-9.
54. Lucklum R, Behling C, Cernosek RW, Martin SJ. Determination of complex shear modulus with thickness shear mode resonatos.J Appl Phys D 1997; 30: 346-356.
55. Granstaff VE, Martin SJ. Characterization of a thickness-shear-mode quartz resonator with multiple non piezoelectric layers. J Appl Phys 1994; 75: 1314-29.
56. Cernosek R, Martin SJ, Hillman AR, Bandey HL. Comparison of lumped-element and transmission-line models for thickness-shear-mode quartz

resonator sensors. IEEE Trans. Ultrason., Ferroelect., Freq. Control. Aug 1998; 45: 1399-1407.

57. Rosenbaum JF. Bulk Acoustic Wave Theory and Devices. Boston, MA: Artech House, 1988.
58. Sauerbrey G. use of quartz vibrator for weighing thin films on a microbalance. J Z Phys 1959; 155: 206-10.
59. Kanazawa KK, Gordon JG. Frequency of a quartz microbalance in contact with a liquid. J Anal Chem Acta 1985; 57:1770-1.
60. Saber R, Mutlu S, Piskin E. Glow-discharge treated piezoelectric quartz crystals as immunosensors for HAS detection. J Biosens Bioelectron 2002; 17: 727-34.
61. Wang H, Lei C, Li J, *et al.* A piezoelectric immunoagglutination assay for Toxoplasma gondii antibodies using gold nanoparticles. J Biosens Bioelectron 2004; 19: 701-9.
62. Su CC, Wu TZ, Chen LK, Yang HH, Tai DF. Development of immunochips for the detection of dengue viral antigens. J Anal Chim Acta; 2003: 479: 117-23.
63. Arnau A, Sogorb T, Jimenez Y. A continuous motional series resonant frequency monitoring circuit and a new method of determining Butterworth-Van Dyke parameters of a quartz crystal microbalance in fluid media. Rev Sci Instrum 2000; 71: 2563-71.
64. Martin SJ, Granstaff VE, Frye C. Characterization of a quartz crystal microbalance with simultaneous mass and liquid loading. J Anal Chem Acta 1991; 63: 2272-81.
65. Bund A, Schwitzgebel G. Viscoelastic properties of low-viscosity liquids studied with thickness-shear mode resonators. J Anal Chem Acta 1998; 70: 2584-8.
66. Aizawa H, Kurosawa S, Ogawa KI, *et al.* Conventional diagnosis of C-reactive protein in serum using latex piezoelectric immunoassay. J Sensors and Actuators B 2001; 76: 173-6.

67. Bilitewski U. Biosensors for environmental monitoring. Bilitewski U., Turner APF (eds). Harwood academic publishers, Amsterdam, The Netherlands: 87-122.
68. Horisberger M, Cleark MF. Labeling of colloidal gold with Protein A. Histochemistry 1985; 82: 219-23.
69. Chu X, Lin Z, Shen G, Yu R. Kinetic studies of immunoglobulin M immunoreaction using quartz crystal microbalance methodology. J Chin Chem Univ 1996; 17: 1025-9.
70. Claycomb RW, Delwiche Mj, Munro CJ, BonDurant RH. Rapid enzyme immunoassay of bovine progesterone. J Biosens Bioelectron 1998; 13(11): 1165-71.
71. baerdemaeker J, Decuypere E, Sansen W. A biosensor to detect penicillin residues in food. Transactions of the ASAE 2000; 43(1): 153-9.
72. Uttenthaler E, Kosslinger C, Drost S. Quartz crystal biosensor for detection of African Swine Fever disease. J Analyt Chim Acta 1998; 362(1): 91-100.
73. Shay M, Bruckenstein S,. Determination of Hg(I) adsorption accompanying the coulostatic underpotential deposition of mercury on gold using the quartz crystal microbalance. J Langmuir 1989; 5.
74. Buttry DA, Ward MD. Measurement of intercial processes at electrode surfaces with the electrochemical quartz crystal microbalance. J Chem Rev, 1992; 92: 1355-79.
75. Fredriksson C, Kihlman S, Rodahl M, Kasemo B. The piezoelectric quartz crystal mass and dissipation sensors: a means of studing cell adhesion. J Langmuir 1998; 14: 248-51.
76. Andres RT, Narayanaswamy R, Fibre-optic pesticide biosensor based on covalently immobilized acetylcholinesterase and thymol blue. J Talanta 1997; 44: 1335-52.
77. Che YH, Yang ZP, Li YB, Paul D, Slavik M. Rapid detection of *Salmonella typhimurium* using an immunoelectrochemical method coupled with immunomagnetic separation. J Rapid Methods and Automation in Microbiology 1999; 7(1): 47-59.

78. Haupt K, Mosbach K. Molecularly imprinted polymers and their use in biomimetic sensors. J chem. Rev 2000; 100(7): 2495-504.
79. Mellgren C, Sternesjo A, Hammer P, Suhren G, Bjorck L, Heeschen W. Comparison of biosensor, microbiological, immunochemical and physical methods for detection of sulfamethazine residues in raw milk. J Food Protection 1996; 59(11): 1223-6.
80. Buttry DA, Ward MD. Measurement of interfacial processes at electrode surfaces with the electrochemical quartz crystal microbalance. J Chem Rev 1992; 92: 1355-79.
81. Xavier MP, Vallejo B, Marazuela MD, Moreno Bondi MC, Baldini F, Falai A. Fiber optic monitoring of carbamate pesticides using porous glass with covalently bound chlorophenol red. J Biosens Bioelectron 2000; 14(2): 895-905.
82. Le D, Feng H, Tai J, Lihua N, Yao S. A goat anti-human modified piezoimmunosensor for *Staphylococcus aureus* detection; J Micro Methods 1996; 23: 229-34.
83. Wang J, DNA biosensors based on Peptide Nucleic Acid (PNA) recognition layers. J Biosens Bioelectron 1998; 13: 752-62.
84. Tombelli S, Mascini M, Sacco C, Turner Anthony PF. A DNA Piezoelectric Biosensor Assay Coupled with a Polymerase Chain Reaction for Bacterial Toxicity determination in Environmental Samples. J Analyt Chim Acta 2000; 418: 1-9.
85. Ketterer T, Stadler H, Rickert E, Bayer E, Gopel W. Detection of Oligonucleotide Sequences with Quartz Crystal Oscillators. J Sensor and Actuators B 2000; 65: 73-5.
86. Tombelli S, Mascini M, Braccini L, Anichini M, *et al.* Coupling of a DNA piezoelectric biosensor and polymerase chain reaction to detect apolipoprotein E polymorphism. J Biosens Bioelectron 2000; 15: 363-70.
87. Kurosawa S, Aizawa H, *et al.* Immunosensors using a quartz crystal microbalance. J Meas Sci Technol 2003; 14: 1882-7.
88. Yang CF, Pen T, Schmalzel J. Design of a Piezoelectric Gene-sensor Using Base-specific Drug-functionalized Nanomicrospheres as Amplifying Probes

Sensors for Industry Conference, New Orleans, Louisiana, USA. January 2004; 27-9.

89. Su XL and Li Y. A QCM immunosensor for Salmonella detection with simultaneous measurements of resonant frequency and motional resistance. J Biosens Bioelectron 2005; 21: 840-8.
90. Chu X, Zhao ZL, Shen GL, Yu RQ. Quartz crystal microbalance immunoassay with dendritic amplification using colloidal gold immunocomplex. J Sensors and Actuators B 2005; 114(2): 696-704.
91. Janshoff A, Steinem C, Sieber M, J Eur Biophys 1997; 26:261.
92. Lee SH, Stubbs DD, Cairney J, Hunt WD. Rapid Detection of Bacterial Spores Using a Quartz Crystal Microbalance (QCM) Immunoassay. IEEE sensors 2005; 5: 737-43.
93. Janshoff A, Galla HJ, Steinem C. Biochemical Applications of Solid Supported Membranes on Gold Surfaces: Quartz Crystal Microbalance and Impedance Analysis. J Eur Biophys 1996; 25:105.
94. Horowitz P, Hill W. THE ART OF ELECTRONICS. 2nd 1989; 284-300.
95. Frerking ME. CRYSTAL OSCILLATOR DESIGN AND TEMPERATURE COMPENSATION. Van Nostrand Reinhold Company, NY.
96. Babacan S, Pivarnik P, Letcher S, Rand AG. Evaluation of antbody immobilization methods for piezoelectric biosensor application. J Biosens Bioelectron 2000; 15: 615-21.
97. Wu TZ, Su CC, Chen LK, Yang HH, Tai DF, Peng KC. Piezoelectric immunochip for the detection of dengue fever in viremia phase. J Biosens Bioelectron 2005; 21: 689-95.

# APPENDIX

## Table 1: Validation of Protein A Concentration

| Conc. of Protein A mg/ml | Freq. (baseline) MHz | Freq. of Protein A MHz | ΔF MHz | Mean of ΔF MHz |
|---|---|---|---|---|
| 0.25 | 12.132928 | 12.132838 | -0.000090 | |
| 0.25 | 12.129426 | 12.129340 | -0.000086 | -0.000088 |
| 0.50 | 12.126995 | 12.126928 | -0.000067 | |
| 0.50 | 12.129547 | 12.129446 | -0.000101 | -0.000084 |
| 0.75 | 12.058020 | 12.057938 | -0.000082 | |
| 0.75 | 12.130460 | 12.130372 | -0.000088 | -0.000085 |
| 1.00 | 12.131917 | 12.131773 | -0.000144 | |
| 1.00 | 12.130976 | 12.130870 | -0.000106 | -0.000125 |
| Bare Crystal No.1 | 12.136331 | 12.136344 | 0.000013 | |
| Bare Crystal No.2 | 12.131398 | 12.131413 | 0.000015 | 0.000014 |
| | | | | |

## Table 2: Validation of Protein A Concentration

| Conc. of Protein A mg/ml | Freq. (baseline) MHz | Freq. of Protein A MHz | ΔF MHz | Mean of Mass $mg/cm^2$ |
|---|---|---|---|---|
| 0.25 | 12.132928 | 12.132838 | -0.000090 | 32.65 |
| | 12.129426 | 12.129340 | -0.000086 | |
| 0.50 | 12.126995 | 12.126928 | -0.000067 | 31.18 |
| | 12.129547 | 12.129446 | -0.000101 | |
| 0.75 | 12.058020 | 12.057938 | -0.000082 | 31.73 |
| | 12.130460 | 12.130372 | -0.000088 | |
| 1.00 | 12.131917 | 12.131773 | -0.000144 | 46.38 |
| | 12.130976 | 12.130870 | -0.000106 | |
| Bare Crystal 1 | 12.136331 | 12.136344 | 0.000013 | -5.19 |
| Bare Crystal 2 | 12.131398 | 12.131413 | 0.000015 | |
| | | | | |

## Table 3: Incubation Time of Ab 2 h

| | Conc. of Ab mg/ml | Freq.(baseline) MHz | Freq.(final) MHz | ΔF MHz |
|---|---|---|---|---|
| **No rotate** | 0.13 | 12.120906 | 12.120779 | -0.000127 |
| **Rotation** | 0.13 | 12.120429 | 12.119959 | -0.000470 |
| **No rotate** | 0.16 | 12.123375 | 12.123202 | -0.000173 |
| **Rotation** | 0.16 | 12.122343 | 12.121798 | -0.000545 |

## Table 4: Incubation Time of Ab 2 h

| Detail | Conc. of Ab mg/ml | freq.(baseline) MHz | freq.(final) MHz | Mean of Mass $mg/cm^2$ |
|---|---|---|---|---|
| **No rotate** | 0.13 | 12.120906 | 12.120779 | 47.21 |
| **Rotation** | 0.13 | 12.120429 | 12.119959 | 174.71 |
| **No rotate** | 0.16 | 12.123375 | 12.123202 | 64.28 |
| **Rotation** | 0.16 | 12.122343 | 12.121798 | 202.53 |

## Table 5: Incubation Time of Antibody Immobilization

| 0.5 h | | 1.0 h | | 2.0 h | | 4.0 h | | 8.0 h | |
|---|---|---|---|---|---|---|---|---|---|
| **1** | **2** | **3** | **4** | **5** | **6** | **7** | **8** | **9** | **10** |
| 205 | 244 | 304 | 303 | 378 | 405 | 279 | 308 | 57 | 164 |
| ΔF = 225 Hz | | ΔF = 304 Hz | | ΔF = 392 Hz | | ΔF = 294 Hz | | ΔF = 110 Hz | |

## Table 6: Validation of Antibody [0.050-0.200 mg/ml]

| No | Conc. of Ab mg/ml | freq. (baseline) MHz | freq. (final) MHz | ΔF MHz | Mean of freq. MHz |
|---|---|---|---|---|---|
| 1 | 0.200 | 12.127322 | 12.126913 | -0.000409 | -0.000451 |
| 2 | | 12.132795 | 12.132302 | -0.000493 | |
| 3 | 0.150 | 12.128210 | 12.127780 | -0.000430 | -0.000410 |
| 4 | | 12.056142 | 12.055728 | -0.000414 | |
| 5 | | 12.135310 | 12.134925 | -0.000385 | |
| 6 | 0.100 | 12.057682 | 12.057308 | -0.000374 | -0.000308 |
| 7 | | 12.127110 | 12.126843 | -0.000267 | |
| 8 | | 12.137442 | 12.137159 | -0.000283 | |
| 9 | 0.075 | 12.047995 | 12.047674 | -0.000321 | -0.000303 |
| 10 | | 12.125751 | 12.125451 | -0.000300 | |
| 11 | | 12.125349 | 12.125062 | -0.000287 | |
| 12 | 0.050 | 12.057394 | 12.057056 | -0.000338 | -0.000382 |
| 13 | | 12.130315 | 12.129889 | -0.000426 | |
| 14 | Blank | 12.053122 | 12.052836 | -0.000286 | -0.000209 |
| 15 | | 12.130177 | 12.130046 | -0.000131 | |
| 16 | Negative | 12.056852 | 12.056572 | -0.000280 | -0.000297 |
| 17 | | 12.125846 | 12.125563 | -0.000283 | |
| 18 | | 12.053906 | 12.053577 | -0.000329 | |

## Table 7: Validation of Antibody [0.050-0.200 mg/ml]

| No | Conc. of Ab mg/ml | freq. (baseline) MHz | freq. (final) MHz | Mean of Mass $mg/cm^2$ |
|---|---|---|---|---|
| 1 | | 12.127322 | 12.126913 | |
| 2 | 0.200 | 12.132795 | 12.132302 | 167.38 |
| 3 | | 12.128210 | 12.127780 | |
| 4 | | 12.056142 | 12.055728 | |
| 5 | 0.150 | 12.135310 | 12.134925 | 152.65 |
| 6 | | 12.057682 | 12.057308 | |
| 7 | | 12.127110 | 12.126843 | |
| 8 | 0.100 | 12.137442 | 12.137159 | 114.84 |
| 9 | | 12.047995 | 12.047674 | |
| 10 | | 12.125751 | 12.125451 | |
| 11 | 0.075 | 12.125349 | 12.125062 | 112.93 |
| 12 | | 12.057394 | 12.057056 | |
| 13 | 0.050 | 12.130315 | 12.129889 | 142.53 |
| 14 | | 12.053122 | 12.052836 | |
| 15 | Blank | 12.130177 | 12.130046 | 78.06 |
| 16 | | 12.056852 | 12.056572 | |
| 17 | | 12.125846 | 12.125563 | |
| 18 | Negative | 12.053906 | 12.053577 | 111.31 |

## Table 8: Validation of Ab [0.0125-0.0500 mg/ml]

| No | Conc. of Ab mg/ml | freq. (baseline) MHz | freq. (final) MHz | ΔF MHz | Mean of freq. MHz |
|---|---|---|---|---|---|
| 1 | 0.0125 | 12.129957 | 12.129694 | -0.000263 | -0.000306 |
| 2 | | 12.056198 | 12.055849 | -0.000349 | |
| 3 | 0.0250 | 12.052575 | 12.052256 | -0.000319 | -0.000310 |
| 4 | | 12.133958 | 12.133657 | -0.000301 | |
| 5 | 0.0500 | 12.129296 | 12.128968 | -0.000328 | -0.000336 |
| 6 | | 12.138566 | 12.138203 | -0.000363 | |
| 7 | | 12.136137 | 12.135820 | -0.000317 | |

## Table 9: Validation of Ab [0.0125-0.0500 mg/ml]

| No | Conc. of Ab mg/ml | freq. (baseline) Hz | freq. (final) Hz | Mean of Mass $mg/cm^2$ |
|---|---|---|---|---|
| 1 | 0.0125 | 12.129957 | 12.129694 | 114.37 |
| 2 | | 12.056198 | 12.055849 | |
| 3 | 0.0250 | 12.052575 | 12.052256 | 115.78 |
| 4 | | 12.133958 | 12.133657 | |
| 5 | 0.0500 | 12.129296 | 12.128968 | 124.61 |
| 6 | | 12.138566 | 12.138203 | |
| 7 | | 12.136137 | 12.135820 | |

**Table 10: Relationship between Conc. of *V. cholerea* O1 and Freq. shift**

| No | *V. cholerae* O1 CFU/ml | freq.(baseline) MHz | freq.(final) MHz | ΔF MHz | Mean of freq. MHz |
|---|---|---|---|---|---|
| 1 | $10^7$ | 12.131629 | 12.130663 | -0.000966 | -0.000837 |
| 2 | | 12.127344 | 12.126636 | -0.000708 | |
| 3 | $10^6$ | 12.057015 | 12.056417 | -0.000598 | -0.000775 |
| 4 | | 12.057927 | 12.056974 | -0.000953 | |
| 5 | $10^5$ | 12.126770 | 12.126081 | -0.000689 | -0.000601 |
| 6 | | 12.056177 | 12.055664 | -0.000513 | |
| 7 | $10^4$ | 12.126709 | 12.126218 | -0.000491 | -0.000476 |
| 8 | | 12.057179 | 12.056717 | -0.000462 | |
| Blank 1 | 0 | 12.054522 | 12.054106 | -0.000416 | -0.000416 |
| Blank 2 | 0 | 12.055226 | 12.05481 | -0.000416 | |

## Table 11: Relationship between Conc. of *V. cholerea* O1 and Freq. shift

| No | *V. cholerea* O1 CFU/ml | freq.(baseline) MHz | freq.(final) MHz | Mean of Mass mg/cm$^2$ |
|---|---|---|---|---|
| 1 | $10^7$ | 12.131629 | 12.130663 | 310.66 |
| 2 | | 12.127344 | 12.126636 | |
| 3 | $10^6$ | 12.057015 | 12.056417 | 291.29 |
| 4 | | 12.057927 | 12.056974 | |
| 5 | $10^5$ | 12.126770 | 12.126081 | 224.29 |
| 6 | | 12.056177 | 12.055664 | |
| 7 | $10^4$ | 12.126709 | 12.126218 | 177.94 |
| 8 | | 12.057179 | 12.056717 | |
| Blank 1 | 0 | 12.054522 | 12.054106 | 156.33 |
| Blank 2 | | 12.055226 | 12.05481 | |

# BIOGRAPHY


| | |
|---|---|
| **NAME** | Miss Warat Chongpermpornwattana |
| **DATE** | 10 March 1976 |
| **PLACE OF BIRTH** | Patchaboon, Thailand |
| **INSTITUTIONS ATTENDED** | Changmai University, 1993-1996<br>Bacherlor of Science<br>(Medical Technology)<br>Mahidol University, 2003-2006<br>Master degree of Engineering<br>(Biomedical Engineering) |
| **HOME ADDRESS** | 180 Ronnakit road, Lomsak, Petchaboon<br>Thailand 67110 |
| **E-MAIL ADDRESS** | fangbiomed@hotmail.com |